MICROBIAL ABUNDANCE AND DIVERSITY IN RESPONSE TO NUTRIENT ADDITION IN SUBSEAFLOOR OCEAN CRUST AT ATLANTIS BANK, SOUTHWEST INDIAN RIDGE

A Thesis

by

Shu Ying Wee

Submitted to the Office of Graduate and Professional Studies of
Texas A&M University
in partial fulfillment of the requirements for the degree of

MASTER OF SCIENCE

Chair of Committee, Jason B. Sylvan

Committee Members, Jessica Labonté
Shari Yvon-Lewis

Head of Department, Shari Yvon-Lewis

August 2019

Major Subject: Oceanography

ABSTRACT

Olivine in the presence of seawater will undergo a reaction known as serpentinization to form the mineral serpentine in addition to hydrogen, methane, and short chain hydrocarbons, which can be metabolized by microorganisms. Environments where serpentinization reactions occur are therefore hypothesized to support microbial life. The goal of the International Ocean Discovery Program (IODP) Expedition 360 (X360) was to recover a representative transect of the lower oceanic crust formed at Atlantis Bank, an oceanic core complex on the southwest Indian Ridge. Recovered cores were primarily gabbro and olivine gabbro, which may potentially host serpentinization reactions and associated microbial life. The goal of this thesis project was to quantify *in situ* microbial cells, analyze the microbial community structure of the *in sit*u rock samples, and assess if nutrient supply influences the microbial community and methane production using a nutrient addition incubation approach. It was found that the microbial cell abundance is positively correlated to vein presence in rocks for certain depths. Microbial community diversity, assessed via 16S rRNA amplicon analysis, was extremely variable with depth. Additionally, different nutrient treatments added to incubations from twelve depths did not have an observable effect on the microbial diversity or methane production. Knowledge gained here will be useful in connecting microbial ecology in deep subseafloor basement to other marine and subsurface habitats. Altogether, the interdisciplinary approach used here provides a peek into life in the subseafloor upper ocean crust.

ACKNOWLEDGEMENTS

I would like to thank my committee chair, Dr. Sylvan, and my committee members, Dr. Labonté, Dr. Yvon-Lewis, and collaborator Dr. Edgcomb for their guidance and support throughout the course of this research.

Thanks also go to my friends and colleagues and the department faculty and staff for making my time at Texas A&M University a great experience.

I would also like to thank my father, Wee Tiat Eng, my mother, Tan Suat Hong, my aunt, Sally Gadoua, and to my siblings Wee Soon Nan and Wee Shu Ern, for their encouragement and love.

Finally, thank you to my friends Heather Lizethe Pendleton, Athena Sagadevan, Nuraslinda Anuar, Shahd Aljandal and Fernando Unyen for their endless support and love.

CONTRIBUTORS AND FUNDING SOURCES

Contributors

This work was supervised by a thesis committee consisting of Dr. Jason B. Sylvan and Dr. Shari Yvon-Lewis of the Department of Oceanography at Texas A&M University College Station, and Dr. Jessica M. Labonté of the Department of Marine Biology, Texas A&M University Galveston.

Part of the 16S rRNA data analyzed for this thesis was provided by Dr. Virginia Edgcomb's lab of Woods Hole Oceanographic Institute. Methane measurements for this project were done in collaboration with Dr. Shari Yvon-Lewis' lab.

All other work conducted for the thesis (or) dissertation was completed by the student independently.

Funding Sources

This work was made possible by National Science Foundation (NSF) OCE Award 1658031, two awards from the United States Science Support Program, and the IODP. Its contents are solely the responsibility of the authors and do not necessarily represent the official views of the TAMU-CS, TAMUG or the NSF.

TABLE OF CONTENTS

Page

LIST OF FIGURES

LIST OF TABLES

1. INTRODUCTION

Serpentinization is the aqueous alteration process of ultramafic rocks such as olivine and pyroxene in the presence of water. Olivine is a magnesium iron silicate mineral with the formula $(Mg,Fe)_2SiO_4$ as its repeating unit, and pyroxenes have the general formula (Ca, Mg, Fe)Si_2O_6 (Smith, 1999). Olivine in the presence of seawater will undergo a reaction (Equation 1) to form serpentine, hydrogen, methane, and short chain hydrocarbons, which can be metabolized by microorganisms (Kelley et al., 2005; Martin et al., 2008; Schrenk et al., 2013).

$$(Mg,Fe)_2SiO_4 + H_2O + C \rightarrow Mg_3SiO_5(OH)_4 + Mg(OH)_2 + Fe_3O_4 + H_2 + CH_4 + C_2\text{-}C_5 \quad (1)$$

Olivine Water Carbon Serpentine Mg-hydroxide Iron(ii,iii) oxide Hydrogen Methane Hydrocarbons

Rocks such as olivine and pyroxene are characteristic of the lower oceanic crust and upper mantle. Serpentinization occurs in numerous settings on Earth, including subduction zones, mid-ocean ridges, and ophiolites. Generally, serpentinization occurs where tectonic processes expose the upper mantle that has been uplifted, and it may also occur in parts of the Earth's subsurface, though constrained by the depths of fluid circulation (Schrenk et al., 2013).

The Lost City Hydrothermal Field (LCHF), an off-axis vent field roughly 15 km away from the spreading axis of the Mid-Atlantic Ridge, is one of the most intensively studied sites of active serpentinization, with alkaline (pH 9.0-9.8) venting fluids between 40-91°C that are rich in hydrogen and methane (Kelley et al., 2005, 2001). The hydrogen produced through serpentinization at LCHF stimulates the metabolic activity of microbes found on the chimney biofilms as well as venting fluids (Brazelton et al., 2011, 2006). Phylogenetic analyses of metagenomic data from LCHF chimneys and terrestrial serpentinite-hosted alkaline seeps at Tablelands Ophiolite, Newfoundland, revealed a high proportion of Betaproteobacteria sequences

that were likely to be H_2-oxidizers (Brazelton et al., 2012). Chimney fluids at LCHF were also found to have microbial communities of low diversity that were dominated by a methane-metabolizing archaeal phylotype termed Lost City Methanosarcinales (Schrenk et al., 2004).

In addition to sites like LCHF, serpentinization also occurs at slow and ultraslow spreading mid-ocean ridges. On ultraslow spreading ridges, the mantle is exposed asymmetrically along the spreading axes and peridotite, the dominant component of the upper mantle, can be found exposed at the seafloor (Cannat et al., 2006; Dick et al., 2003; Michael et al., 2003). The Southwest Indian Ridge (SWIR) is a major plate boundary that separates the Antarctic and African continent and extends from the southern Atlantic Ocean to the Indian Ocean. The SWIR is one of the two slowest spreading ridges in the world with a full spreading rate of ~14mm/year (at 28˚S, 64˚E), varying only slightly along the 7700 km ridge axis; the Gakkel ridge in the Arctic Ocean is the only other ultraslow spreading ridge (Dick et al., 2016, 2003). Atlantis Bank lies 73 km south of the ultraslow spreading SWIR (Figure 2), exposing the largest known gabbro complex in the oceans (660km^2), ~ 700m below sea level, providing convenient drilling access to an otherwise largely inaccessible environment. To learn about the structure of lower oceanic crust and to study the deep subseafloor biosphere in this underexplored biome, IODP Expedition 360 drilled Hole U1473A at Atlantis Bank from 30 November 2015 through 30 January 2016. Hole U1473A is located at 32°42.36'S, 57°16.68'E (Figure 2) and was drilled to a depth of 789.8 mbsf. 469.4m of core was recovered, with an average of 59% recovery over the entire interval (>96% over the lower 200m of the hole), making it the deepest igneous rock penetration from the seafloor during a single scientific ocean drilling expedition to date (Dick et al., 2016). Hole U1473A cores are composed of a variety of gabbroic lithologies, from primitive olivine gabbros to evolved oxide-rich gabbros (Dick et al.,

2016). This composition provides the necessary elements for serpentinization. The electron donors such as H_2 and CH_4 that are released from serpentinization can be harvested by microorganisms for metabolic energy (Schrenk et al., 2013). Therefore, sites where serpentinization is active or likely to occur in the Atlantis Bank subsurface may support microbial populations utilizing the carbon source provided by water-rock reactions.

The microbiology of ultraslow spreading ridges not been extensively studied at either Gakkel ridge or the SWIR, though microbial communities have been discovered at the hydrothermal systems along the ridges, as well as in the sediments (Chen and Shao, 2008; Ding et al., 2017; Kröncke et al., 1994; Li et al., 2013; Takai et al., 2004). The two sites where the deepest holes have been drilled into the lower crust of a slow and an ultraslow spreading ridge are at Atlantis Bank, at the SWIR; and at the Atlantis Massif core complex, along the Mid-Atlantic Ridge at 30N (Hole U1309D). Hole 1309D was drilled during IODP Expeditions 304 and 305 also in an effort to recover a complete section of the lower ocean crust and uppermost mantle (Blackman et al., 2011, 2006).

Recently, IODP Expedition 357 employed shallow drilling (≤16mbsf) at 7 sites to explore subseafloor life linked to serpentinization at Atlantis Massif (Früh-Green et al., 2018); preliminary results show that cell counts for the sites ranged from 10 to 10^3 cells/cm^3, with some of the basement samples below the minimum quantification limit of 9.8 cells/cm^3. Previous work investigating the microbial diversity of the subseafloor gabbro below Atlantis Massif revealed Proteobacterial lineages closely related to known hydrocarbon degraders. Evidence from functional gene analyses also supported the potential for hydrocarbon degradation, despite the

microbial community being generally low in diversity (Mason et al., 2010). However, that site is younger and warmer and represents the warmer end-member of serpentinizing systems. Quantification of microbes in subseafloor basement conducted at North Pond found the detection limit to be ~10^3cells/cm^3, and the microbial abundances for basalt in the basement ranged from below detection to $6.1*10^4$ cells/cm^3, with the range for samples where cell abundance was above detection being were between $1.0*10^3$ and $6.1*10^4$ cells/cm^3 (Zhang et al., 2016). The samples collected during Expedition 360 provide an unprecedented opportunity to study the microbial communities at much greater depths and on an older, inactive massif, which is likely representative of a larger volume of oceanic basement than the still active Atlantis Massif. The samples also allow for comparison to the pioneering work of Mason and colleagues using modern molecular biology techniques that were not available at the time of their work (Mason et al., 2010). Determining the microbial abundance as a function of depth will also allow us to understand if the presence of fluid flow in the rocks affect the microbial population along the 790 m core. Among the gabbroic basement samples obtained from the core, certain depths show signs of fluid flow and low-temperature hydrothermal alteration, as indicated by the presence of felsic veins, carbonate veins or clay minerals. Carbonate veins are veins in the rocks where seawater has percolated through, and felsic veins are veins in the rocks that were originally formed by flow of magma. The cell counts from depths with evidence of fluid flow are postulated to be greater than counts from depths without the presence of veins.

The volume of habitable subsurface igneous basement is potentially as large as the marine water column, with populations predicted to rival or exceed those of marine subsurface sedimentary biomass (Heberling et al., 2010; Kallmeyer et al., 2012), although the few data points available for

basement cell counts indicate lower population density than sediments and the water column (Jungbluth et al., 2013; Zhang et al., 2016). While the presence of microbial life in the subsurface biosphere was first detected in the 1990's (Parkes et al., 1994), modern molecular biology methods were introduced only more recently to study these environments (Biddle et al., 2008; Cowen et al., 2003; Inagaki et al., 2015, 2006; Mason et al., 2010; Orsi et al., 2013). With the notable exception of the Juan de Fuca Ridge (JdFR) (Cowen et al., 2003; Jungbluth et al., 2013; Lever et al., 2013; Smith et al., 2011) and Louisville seamounts in the Pacific ocean (Sylvan et al., 2015) and Atlantis Massif (Früh-Green et al., 2018; Mason et al., 2010) and North Pond in the Atlantic Ocean (Jørgensen and Zhao, 2016; Meyer et al., 2016; Zhang et al., 2016), recent IODP expeditions have primarily focused on studying microbial communities in sediments. Quantification of microbes in subseafloor basement have been conducted at sites described earlier such as North Pond and Atlantis Massif and this collectively yields only a preliminary peek at the heterogeneity in the global population. The core samples from the Expedition 360 thus present an opportunity to expand the study of the microbial basement biosphere by including samples from the Indian Ocean. Quantifying abundance in the subseafloor crust and identifying the microbial community present, particularly at a site such as U1437A, that is representative of basement rock samples from a serpentinizing environment at an ultraslow spreading ridge in the Indian Ocean, can improve our understanding of the microbial life present in the lower oceanic crust.

2. OBJECTIVES AND ASSOCIATED HYPOTHESES

2.1 - Quantification of cell abundance from core samples

Hypothesis 1: Microbial abundance along the core is positively correlated to the presence of indicators of fluid flow and hydrothermal alterations such as carbonate veins or felsic veins.

2.2 – Assessment of microbial community and diversity from *in situ* core samples via analysis of the 16S rRNA gene

Hypothesis 2: In situ microbial community structure and diversity is positively correlated to the number of veins.

2.3 - Determine if nutrient supply controls microbial diversity and methane production using a nutrient addition incubation approach

Hypothesis 3: Added nutrients will stimulate diversity in microbial communities.

Hypothesis 4: Additions of lactate, acetate and formate will enhance methane production.

3. METHODS

3.1 - Sample collection

Onboard IODP Expedition 360, rock sample selection and preparation were done by Jason Sylvan and Virginia Edgcomb. Whole-round sections were selected from whole-round core samples for dedicated microbiology investigation and then transferred into a sterile Whirlpak bag and transported to the microbiology laboratory for processing. Once in the microbiology laboratory, the whole-round sample was rinsed four times in sterile water (changing the Whirlpak bag once after the second rinse) to reduce contamination from drilling fluid. The sample was then transferred to an ethanol-sterilized metal rock box placed within a positive pressure clean area. The outside of each core was sprayed with 75%–95% ethanol, wiped with Kimwipes, and then sprayed one final time with ethanol and left to air dry (~5 min). During the drying time, photographs of each side of the whole-round sample were taken while it was sitting in the rock box. At all stages of the process, samples were handled as little as possible and with gloved hands only. After cleaning the exterior of whole-round core samples, the rock was split with a sterile chisel and core interiors were subsampled for off-shore investigations mentioned in this project such as cell counts, enrichment cultures and DNA extraction. It is assumed that the ethanol would not seep into the interior portion of the rock cores that were used for microbiology. Previous work with IODP core samples have employed flame sterilization to sterilize the exterior of the core; it was found that despite utilizing harsh treatments, the flaming was effective at killing cells on the exterior but was not detrimental to cells in the interior (Lever et al., 2006). As the interior of rock cores are generally free from contamination, efforts were taken to sample only the interior of the cores. Sections that showed some sign of alteration or fluid flow conduits were specifically chosen because these are the most likely locations for microbial life. Microbiology samples on average were 10–20 cm long.

3.2- Cell Separation and Counts

In order to accurately quantify the cells along the core, an intricate cell extraction that maintains the intactness of cells while successfully separating them from the rock surfaces and therefore allowing for collection on a filter and subsequent quantification via fluorescence microscopy was used. This is a modified version of a cell extraction and enumeration method developed for quantifying microbial abundance in subseafloor sediments (Morono et al., 2013) that was adapted for samples from ocean crust. Samples were powderized in a diamonite mortar and pestle that was decontaminated with 70% EtOH, and then fixed in sterile filtered 2% formaldehyde at a volume:volume ratio of 1:5. For each cell separation run, 1 mL of the fixed sample slurry was first placed into a 15 mL centrifuge tube. Then, 1.4 mL of 2.5% NaCl, 300 µL of detergent mix (100 mM EDTA, 100 mM sodium pyrophosphate, 1% [v/v] tween-80), and 300 µL of pure methanol were added. The samples were then shaken at 500 rpm for 60 min, followed by 40 cycles of sonication at 160 W for 30 seconds, followed by 30 seconds of rest. Following shaking and sonication, the samples were applied onto a density gradient in a new 15 mL tube containing layers composed, from top (least dense) to bottom (most dense), of 30% Nycodenz (1.15 g/cm^3), 50% Nycodenz (1.25 g/cm^3), 80% Nycodenz (1.42 g/cm^3), and 67% sodium polytungstate (2.08 g/cm^3), which were prepared by overlaying lighter density solutions onto heavy ones. Cells and rock particles were separated by centrifugation at 7064× *g* for 1 hour at 25°C using a swing-arm centrifuge rotor. The powderized rock particles sedimented at the bottom of the tube and the light density supernatant layer that contains microbial cells was carefully collected with a syringe and 20G needle. The heavy fraction, including precipitated sediment particles, was washed by re-suspending with 5 mL of 2.5% NaCl and then centrifuged at 5000× *g* for 15 min at 25°C. Recovered supernatant was placed on the same cell fraction obtained above. Sedimented rocks

then underwent a second round of separation following the same protocol as the first round. Following centrifugation, the light density supernatant layer was collected by using syringe with a 20G needle and added to the previous supernatants. All of the supernatant was then filtered through a 0.22-µm polycarbonate membrane filter, with a 0.45 µM cellulose backing membrane. Cells on the polycarbonate membrane filter were stained with SYBR Green I staining solution (100 µL of 1/40 SYBR Green I in TE buffer).

The number of SYBR Green I-stained cells were enumerated using a Zeiss AxioImager.M2 by counting approximately 400 fields of view if fewer than 40 cells total were detected, or at least 40-50 cells in fewer fields when possible. The limit of quantification was defined as 3X the standard deviation of the mean of the negative control counts, and duplicate counts were done for 13 of the samples for replication. One negative control was processed and analyzed for every eleven experimental samples.

3.3 – Nutrient Addition Incubation Experiments

The nutrient addition experiments allow for the assessment of whether added inorganic nutrients and/or organic carbon can stimulate growth of the *in situ* microbial communities, and if one of those treatments is more effective at stimulating growth, which would indicate that nutrient limitation may occur in the deep subseafloor biosphere. Microcosm experiments in 38 mL serum vials were used for this purpose, with anaerobic artificial seawater (ASW) as the basal media for all enrichments (Table 1) (MacLeod et al., 2017). Four conditions were tested: (1) no added nutrients (NT), (2) +750 µM ammonium chloride (NH_4Cl) (+N), (3) +750 µM NH_4Cl +50 µM potassium phosphate, dibasic (K_2HPO_4) (+NP) and (4) +200 µM each of lactate, acetate, and

formate (+C). To initiate enrichments, ~1 to 5 cc of crushed rock chips, depending on sample availability, were transferred to 30 mL serum vials and submerged in anaerobic ASW to a level equivalent to 27 mL total volume (rocks plus media). After the appropriate additions were made to the vials, they were sealed with butyl stoppers and gassed with a mixture of 90% N_2, 5% H_2, 5% CO_2. Using consistent headspace volume allows for quantitative analysis of methane. A total of 51 vials were incubated; these nutrient addition incubations were kept at 10˚C and were initially sampled for headspace CH_4 roughly six months after beginning the incubation and then again at roughly a year post cruise.

3.4 – Methane Measurements

CH_4 in the headspace of the vials was measured using a Gas Chromatograph with a Flame Ionization Detector (GC-FID) post 25 weeks and 60 weeks of incubation. The gas in the headspace of the vials was extracted and measured using GC-FID, similar to previous protocols (Johnson et al., 1990; Valentine et al., 2010). Calibrations were performed for the measurements using methane tanks at 0 ppm, 1.0 ppm, and 6.41 ppm, and the sample loop was flushed for one minute prior to each calibration measurement. The syringe used to inject the gas samples into the GC-FID loop was flushed three times with the 90 % N_2, 5 % H_2, 5 % CO_2 gas mixture prior to each sample extraction and injection.

3.5 – DNA extraction and 16S rRNA Analysis

Roughly 0.5 cm^3 of rocks from each of the nutrient addition incubation samples were used in the DNA extraction with the MP Biomedical FastDNA® Spin Kit for Soil, where the final elution volume was 50 μL, with varying concentrations of ng DNA/μL. New England Biolabs Inc. Q5®

High-Fidelity DNA Polymerase was used to PCR amplify the V4-V5 region of the 16S rRNA gene with the 515F and 926R primer pair (Parada et al., 2016). Upon completion of extraction and amplification, samples were pooled in equimolar concentrations and analyzed with Illumina MiSeq sequencing (Caporaso et al., 2012; Claesson et al., 2010; Walters et al., 2016) at Georgia Genomics Facility. The sequence reads were analyzed with the DADA2 (Divisive Amplicon Denoising Algorithm 2) pipeline in the R programming language to produce amplicon sequence variants (ASVs). DADA2 utilizes a model-based approach to correct errors in amplicons without constructing operational taxonomic units (OTU) (Rosen et al., 2012). Using the DADA2 workflow, the sequences are inferred exactly, and it can resolve differences of as little as 1 nucleotide. The package itself still implements the full amplicon workflow that includes filtering, dereplication, chimera identification, and merging paired-end reads. ASVs are higher-resolution analogue of the OTU (Callahan et al., 2016). The primary difference between making ASV's and the traditional clustering approach for OTUs is that the unique identical 16S rRNA sequences are first identified prior to downstream analyses for ASVs, whereas when generating OTUs, the sequences are clustered at a certain similarity threshold such as 97%, before downstream analyses (Callahan et al., 2017, 2016).

For unaltered core samples, DNA was extracted and PCR of the V4-V5 region of 16S rRNA conducted as above for 43 samples from Hole U1473A in the lab of collaborator Dr. Virginia Edgcomb at Woods Hole Oceanographic Institution. Amplicons were sequenced at Georgia Genomics Facility, and ASVs were generated as described above to determine *in situ* microbial diversity downcore in Hole U1473A. For core samples that overlap with depths where incubations were performed, the core samples act as the time = 0 samples.

Statistical analyses performed with the 16S rRNA sequences from the incubation samples included plotting a non-metric multidimensional scaling (NMDS) based on pairwise Bray-Curtis dissimilarity. This was made using the vegan and phyloseq package in R (McMurdie and Holmes, 2013; Oksanen et al., 2019). One-way analysis of variance (ANOVA) was also used for analyzing the effect of the different treatments on the diversity of the samples, as well as on methane production. The null hypothesis is that there is no difference between the treatment groups. The null hypothesis is rejected if the p value is <0.05, and if F is greater than F_{crit}. Richness and diversity of the *in situ* and incubation samples were calculated using the software *mothur*, version 1.42.1 (Schloss et al., 2009), the number of ASVs present represents richness, and inverse Simpson values were calculated upon subsampling using *mothur* to represent diversity.

4. RESULTS

4.1 - Cell Abundances along the Core

Cell counts are plotted with respect to depth to illustrate potential correlation between cell abundance and vein frequencies/presence (Figure 3). The limit of quantification is three times the average of the negative control cell counts, which is $9.90*10^1$ cells/cm^3 (black line in Figure 3), shown by the vertical line in the cell count plot. The cell counts had a range from zero to 10^4 cells/cm^3, with an average of $6.1*10^2$ cells/cm^3 for all the samples. Roughly 35% of the cell counts were below the limit of quantification. Correlation coefficients were calculated for all depths, and for depth ranges of every 100m, to obtain a statistical analysis of the relationship between cell abundance, carbonate vein frequency, and felsic vein frequency (Table 2). In addition to comparing the cell abundances to vein frequencies at depth ranges of every 100 m, cell abundances were also compared to vein frequencies at varying depth ranges in order to determine other depth ranges that show a positive correlation (Table 3). Correlation coefficients for 12 varying depth ranges were calculated, and these depth ranges were selected based on highest cell abundances and vein frequencies (Table 3). The depth ranges were chosen to cover at least three cell count data points. From 0 to ~100 mbsf, cell abundances were below the limit of quantification in seven out of eight samples (Fig. 3). No carbonate veins are present in this interval, and there are low felsic vein frequencies. There are high felsic and carbonate vein frequencies from 180-200 mbsf though the cell counts do not correlate positively to these high vein frequencies. The highest cell abundance recorded was $1.73*10^4$ cells/cm^3 at depth 248 mbsf, and both felsic and carbonate vein frequencies were relatively low at this depth. From 280-470 mbsf, and 580-620 mbsf, high vein frequencies were present for both felsic and carbonate veins. Strong positive correlation between cell abundance and vein frequencies were from from 280-470 mbsf. However, cell abundances did

not show a significant increase from depths 580-620 mbsf, despite the highest vein frequencies observed from these depth ranges. In addition, from 300-400 mbsf, most cell abundances were below the limit of quantification. While there are few veins present from 640-720 mbsf, the cell counts still range from 10^2-10^3 cells/cm^3. From 720m to 730m, there is a high felsic vein frequency and the cell counts for that depth corresponds positively to the vein frequency. From Table 2 and 3, most of the relationships have a negligible correlations. Several strong positive correlations were found from four depth ranges: 219 to 248 mbsf, 300 to 333 mbsf, 400 to 500 mbsf, and 500 to 600 mbsf.

4.2 - In situ Samples Microbial Community Analysis

Collaborator Virginia Edgcomb successfully extracted genomic DNA from 43 *in situ* rock samples. The V4-V5 region of the 16S rRNA gene was amplified from all samples and sequencing reads were obtained via Illumina MiSeq sequencing. ASVs were constructed from the Illumina-MiSeq sequences based on the DADA2 pipeline in R (Callahan et al., 2017, 2016). Two quality control steps were applied to the ASVs: i) Removal of ASVs present the samples and in the blank PCR and blank kit control samples, and ii) Removal of ASVs commonly found in PCR contamination. The blank kit control was an empty kit sample that was subjected to same process of DNA extraction. This is done to identify any possible contaminants present in the kit itself. The number of ASVs and reads present before and after both quality control steps are shown in Table 4. A total of 2,829,453 reads were constructed for all samples, including two PCR blank control samples. Upon removing the reads that overlapped between core samples and the control samples, there were 707,132 reads; containing 4,541 ASVs. After removing genera that were commonly

found in PCR contamination (Salter et al., 2014; Sheik et al., 2018), 200,701 reads remained representing 2,649 ASVs.

A total of 83.3% of the sequences were Bacteria, and 16.7% of the sequences were Archaea. The Bacteria sequences were dominated by Proteobacteria, which constituted 50.4% of the sequences, followed by Marinimicrobia (14.8%), Firmicutes (9.0%) and others, defined as lineages which represent Actinobacteria, Bacteroidetes, Firmicutes, Planctomycetes, Verrumicrobia, Fusobacteria, Nitrospinae, Cyanobacteria, Chloroflexi, AncK6, Gemmatimonadetes, Acidobacteria, Lentisphaerae, Margulisbacteria, Dependentiae, PAUC34f, and Nitrospirae (25.8%). The archaeal sequences comprised of three phylum: Thaumarchaeota (77.1%), Euryarchaeota (19.7%), and Nanoarchaeota (3.2%) (Table 5).

The community composition for all *in situ* rock samples at the class taxonomic level are shown in Figure 4. The classes that are below 10% of the sequences are defined as Others. Table 6 presents the phylum and classes for the taxa categorized as Others in Figure 4. The depths with asterisks are the depths that are shared in common with the incubation experiment samples (n= 9). Out of the 43 samples, 3 samples did not have sequences that were present after the screening process; these have been excluded from the bar plot in Figure 4. Two depths (209, and 306.7 mbsf) were comprised of ASVs that could only be classified to the phylum level. Six depths (10.7, 44.5, 91.3, 209, 306.7, 714.9 mbsf) did not have any Archaeal sequences present. While the most abundant class changes with depth, Nitrososphaeria, Alphaproteobacteria, and Gammaproteobacteria are the three classes with high abundances throughout all depths. To gain a better understanding of the microbes present at each depth, the most abundant genera for each depth, other than the ones

classified only to a higher taxonomic level, are listed in Table 7; the most abundant genera vary with depth as well.

Richness and diversity of the samples was calculated with respect to depth using the software *mothur*, version 1.42.1 (Schloss et al., 2009) (Table 8). 1,326 reads were selected as the threshold for subsampling, this was the lower quartile for the number of reads present in all depths. Inverse Simpson values for depths 10.7, 13.9, 91.3, 111.9, 332.8, 375.1, 533.5, and 626.3 mbsf were not calculated as the number of reads in these samples were below this threshold. The depth with the highest richness and diversity was 182.4 mbsf. The depth with the lowest richness was 10.7 mbsf, and the depth with the lowest calculated diversity was 44.5 mbsf. Other notable depths with relatively high richness and diversity are 404.9, 452.9, 600.5, and 711.3 mbsf. The depths with the highest diversity also have the highest richness.

Correlation coefficients were calculated for all depths, and for depth ranges of every 100m, to obtain a statistical analysis of the relationship between diversity, carbonate vein frequency, felsic vein frequency, and total vein frequency (carbonate and felsic vein frequency combined) (Table 9). The correlation coefficient for all depths and total vein frequencies is 0.56, which shows a moderate positive correlation. From depths 0-100 mbsf, there is no correlation between diversity and vein frequencies. For the depths that range from 100-200, 300-400, 400-500, 500-600, 600-700, and 700-800 mbsf, there is a very strong positive correlation between diversity and vein frequencies. From 300-400 mbsf, there is a perfect positive correlation between diversity and vein frequencies, however, it is important to note that only two diversity values are available for that depth range. Three out of the eight depth ranges show a very strong positive correlation between

diversity and carbonate vein frequency, and five out of the eight depth ranges show a very strong positive correlation between diversity and felsic vein frequency.

4.3 - Nutrient Addition Incubation Experiments Community Analysis

Genomic DNA was successfully extracted from all rock samples in the nutrient addition incubation experiments. The V4-V5 region of the 16S rRNA genes was successfully amplified from all samples. The number of ASVs and reads present before and after both quality control steps are shown in Table 10. A total of 202 ASVs and 5,293,213 reads were constructed for all samples including negative control samples (control samples included three PCR blank controls, a blank DNA extraction kit control, and a blank filter control). The blank filter control was made by using a blank 0.2 µm polycarbonate filter that was subjected to the same DNA extraction process as the samples. Upon removing the ASVs that overlapped between the experimental samples and the control samples, there were 594,880 reads. Archaeal 16S rRNA genes were not detected in the nutrient addition experiments. From these 594,880 reads, 173 ASV's were found. After removing ASVs that were commonly found in PCR contamination (Salter et al 2014, Sheik et al 2018), 94 ASVs remained, representing a total of 215,398 sequences.

The samples were dominated by Proteobacteria, which constituted 64.9% of the sequences, followed by Firmicutes (13.8%) Acidobacteria (5.3%), Bacteroidetes (5.3%) and others (10.6%) that include Acidobacteria, Armatimonadetes, Cyanobacteria, Deinococcus-Thermus, Marinimicrobia and Planctomycetes (Table 11). The community composition for all incubation samples for each depth and treatment at the class taxonomic level are shown in Figure 5. The classes that are below 10% of the sequences are defined as Others. Gammaproteobacteria made up

54.1% of the Proteobacteria sequences, while Alphaproteobacteria, Hydrogenophilalia, and Deltaproteobacteria made up 32.8%, 11.5%, and 1.6% of the Proteobacterial sequences respectively.

The community composition for each depth and treatment at the genus taxonomic level is shown in Figure 6. The classes that are below 10% of the sequences are defined as Others. Some ASV's were classifiable only up to a higher taxonomic level than genus, and these were labeled in the figure. The sequences that were only classified to a higher taxonomic level than genus formed the majority of the sequences with a total of 58,620 reads. Apart from these, the five most abundant genera found were *Hydrogenophilus*, RB-41 (environmental sequences representing an uncultured genus within the family Pyrinomonadaceae), *Bacillus*, *Thermicanus*, and *Curvibacter*. There were seven ASVs classified as *Hydrogenophilus,* representing 47,500 reads. Two ASV's were classified as RB-41, representing a total of 31,064 reads. *Bacillus* was represented by four ASVs and 15,164 reads, and five *Thermicanus* ASVs were detected, representing a total of 6,686 reads. *Curvibacter* represented one ASV and a total of 6,311 reads.

Out of the 48 samples, 14 samples did not have sequences that were present after the removal of ASVs that overlapped between the experimental samples and the control samples, as well as common genera found in PCR contamination, these have been removed in the figure, and the removed samples are listed in Table 16.

To determine the richness and diversity of the samples with respect to depth and treatments, the number of ASVs present at each depth is tabulated to represent richness, and inverse Simpson

values were calculated upon subsampling using *mothur* to represent diversity (Table 12). 1,062 reads were selected as the threshold for subsampling, this was the lower quartile for the number of reads present in all samples. Inverse Simpson values for depths in mbsf (with treatments) 247.7-N, 332.8-NP, 420.9-NT, 460.4-NT, 626.3-NP, 639.3-N, 714.9-NP, and 747.7-C were not calculated as the number of reads in these samples were below this threshold. All the samples are low in diversity. The depth and treatment with the highest richness and diversity in relative to the other depths and treatments were 274.6-NP, and 70.9-N respectively.

Richness and inverse Simpson values were also calculated for all incubation samples with respect to depth (all treatments combined) (Table 13). 7,644 reads were selected as the threshold for subsampling, this was the lower quartile for the number of reads present in all depths. Inverse Simpson values for depths 332.8, 421.5, and 639.3 mbsf were not calculated as the number of reads in these samples were below this threshold. The depths with the highest richness are 274.6 mbsf, 70.9 mbsf, and 714.9 mbsf. The depths with the highest diversity relative to other depths are 70.9 mbsf, 228.8, and 274.6. Unlike with the *in situ* samples, increase in richness does not also follow an increase in diversity. There were a few notable similarities in diversity of the samples relative to other depths for the *in situ* and incubation samples. Depth 228.8 mbsf was the only depth to exhibit high diversity relative to the other depths for both *in situ* and incubation samples. Depth 247.7 mbsf showed low diversity in both *in situ* and incubation samples.

To investigate the effect of treatments, the richness and diversity were calculated for all incubation samples with respect to treatments (all depths combined), and this is presented in Table 14. Samples with NP addition showed the highest richness, followed by N addition, C addition and no

treatment. The highest diversity was observed in samples with C addition, followed by NP addition, no treatments, and N addition. Richness did not correspond to increase in diversity. As the inverse Simpson values are similar for the treatments, a one-way or single-factor analysis of variance (ANOVA) was calculated to determine if the values are statistically similar for each treatment group. This was done using the inverse Simpson values calculated in Table 11. The null hypothesis is that there is no difference between the treatment groups. It was found that $p > 0.05$ and $F < F_{crit}$. The null hypothesis is not rejected and the effect of each treatment on the microbial community diversity is not statistically different.

In addition to the treatments being statistically similar in their effect on microbial diversity, there were inconsistencies in the presence of certain genera in the incubation samples. Genera that were highly abundant at a particular depth, would typically be found in only one of the added treatments, but not in the incubation sample without any treatments. For example, at depth 714.9 mbsf, for the N-addition, *Hydrogenophilus* was the most abundant genus, but this genus was only found in the N-addition, and not in the incubations without treatment, or other nutrient additions. Subsequent analyses for the samples were presented as a whole for each depth, and sequences from each treatment were combined.

Figure 7 and 8 respectively depict the microbial community on the class and genus taxonomic level for all 11 depths (all treatments combined). Gammaproteobacteria is the most commonly abundant class for four of the depths: 70.9, 421.5, 460.4, and 626.3 mbsf, followed by Hydrogenophilalia at 274.6, and 747.8 mbsf. At depths 228.8, 247.7, 639.3, and 714.9, the most abundant classes are Alphaproteobacteria, Bacilli, Oxyphotobacteria, and Blastocatellia

respectively. The most abundant genera for each depth vary distinctly (Figure 8). At depths 70.9 and 626.3 mbsf, most of the genera are only classified to a higher taxonomic level. Hydrogenophilus is the only genus that is at top abundance for more than one depth (274.6 and 747.8 mbsf. At depths 228.8, 247.7, 332.8, 421.5, 460.4, 639.3 and 714.9 mbsf, the most abundant genera are Acidovorax, Bacillus, Formosa, Pelomonas, Tepidimonas, Chroococcidiopsis, and RB-41. The closest relatives to the ASV sequences for each genus are briefly described in Table 17.

Figure 9 depicts the NMDS plot to visualize the dissimilarity in microbial community structure among the nutrient incubation samples. The only apparent major clustering of microbial communities is in the center of the plot. All samples from depths 70.9, 626.3, and 714.9 mbsf are present within this grouping, in addition of a high portion of samples with C addition. Microbial communities in C addition treatments showed separation into two groups, where communities from 70.9, 228.8, 460.4 and 714.9 mbsf, that are clustered closer together in the center, are more similar than the communities from depths 274.6, 639.3, and 747.7 mbsf. For N addition, the microbial communities are all different from each other, and the only pairing that is visible are with depths 420.9 and 639.3 mbsf. NP addition communities were mostly clustered together as can be seen in the center, except for four depths that range from 228.8 to 332.8 mbsf. Microbial communities that received no added treatments can be seen mostly on the top half of the plot, though most of the communities are well spread out and are different (depths: 228.8, 247.7, 274.6, 420.9, 460.4, 747.7 mbsf).

4.4 - Methane Measurements from Nutrient Addition Incubation Experiments

No methane measurements were performed onboard the ship at the start of the incubation. It was assumed that the methane concentration at the start of the incubation would be zero. For the blank controls, three negative controls of ASW with no rocks added were measured and the average for methane production after 60 weeks was $2.76*10^{-3}$ nmol/day. The rate at 25 weeks was derived from the value measured at 25 weeks minus the initial value (zero) divided by time elapsed in days. The rate at 60 weeks derived from the difference between methane measured at 60 weeks and methane measured at 25 weeks divided by time elapsed since the 25 weeks measurement. In nearly all the experiment bottles, methane was detected when samples were collected at six months and again after one year of incubation with methane production ranging from zero to as high as 0.1 nmol/day (Figure 10). The average methane production for all samples and treatments after 25 weeks and 60 weeks was $1.7*10^{-2}$ nmol/day and $2.05*10^{-2}$ nmol/day, respectively. Carbonate and felsic vein frequencies are compared to methane activity (Figure 10). Correlation coefficients were determined for both the 25 and 60 weeks methane production rates compared to carbonate and felsic vein frequencies (Table 18). There is a negligible correlation of 25 weeks methane production with both types of veins, but there is a weak positive correlation between 60 weeks methane production with both types of veins.

Based on Figure 10, methane production in the C addition treatments was higher than in the NT samples after 25 weeks for samples from seven depths: 70.9, 91.3, 247.7, 274.6, 421.5, 626.3, 714.9 mbsf. At depths 91.3, 421.5, and 626.3 mbsf, the methane production was not higher in the C-addition than it was in the NP-addition. At depth 714.9, methane production in the N-addition was higher than that in the C-addition.

For methane production after 60 weeks was higher in the C-addition than in the sample without nutrients added for 91.3 and 274.6 mbsf; though NP-addition incubation sample had higher methane production than C-addition. There is no significant trend of increased methane production with increased organic carbon source addition. One-way analysis of variance (ANOVA) was calculated to determine if methane production is statistically similar for each treatment group (Table 19). For methane production at both 25 and 60 weeks, it was found that the effect of each treatment on methane production is not statistically different.

5. DISCUSSION

5.1 – Addressing Hypothesis 1: Microbial abundance along the core is positively correlated to the presence of indicators of fluid flow and hydrothermal alterations such as carbonate veins or felsic veins.

The convective circulation of seawater in the subseafloor aquifer creates a mechanism in which heat and mass can be transferred between the crust and the ocean and by which microbes can be dispersed (Orcutt et al., 2013; Whitman et al., 1998). Fluid flow through the rocks can therefore introduce microbes into subsurface environments, and it was thus hypothesized that the presence of fluid flow or hydrothermal alteration indicators such as veins would correlate positively to cell concentrations. The path left behind by these fluid alterations can create space and pathways in the rocks for microbes to move, obtain nutrients, and colonize. A study done with subsurface samples from North Pond, from the west flank of the Mid-Atlantic Ridge, used quantitative PCR (qPCR) to determine an average cell concentration of 1.4-2.2 * 10^4 cells/g of rock samples (Jørgensen and Zhao, 2016). However, the authors did note that cell estimates based on primer-based approaches are prone to bias and the numbers should be evaluated with this in mind (Jørgensen and Zhao, 2016). The rock samples obtained for the North Pond study were also mainly from igneous crust. Another study of microbial abundance along a 254 m core of basaltic rock at Hole U1383C from North Pond found cell abundances on the same order of magnitude as well, ranging from $1.0*10^3$ to $6.1*10^4$ cells/cm^3 (Zhang et al., 2016). Cell abundances found from the interior portion of basement samples drilled to 57m at Atlantis Massif ranged from <10 to $6.5*10^2$ cells/cm^3 (Früh-Green et al., 2018). Compared to the average cell abundance from the Expedition 360 *in situ* rock samples ($6.10*10^2$ cells/cm^3), the averages from North Pond are much higher, while the average counts for this project is very close to the upper range of cell abundance from Atlantis Massif

basement samples. This could be due to the difference in lithologies as well, where North Pond is hosted by basaltic rocks while lithologies of Atlantis Massif are more similar to that present at Atlantis Bank, with olivine-rich rocks. Highest felsic and carbonate vein frequencies were observed at 180-200 mbsf, 280-470 mbsf, 580-620mbsf, and 720 mbsf. However, cell abundances that were on the higher end (10^3-10^4 cells/cm^3) were only observed at 248 mbsf and 724 mbsf. It is important to note that while high vein frequencies were not indicative of higher cell counts, low vein frequencies were not indicative of lower cell counts either. The distribution of cell abundance had strong positive correlations to vein frequencies at depth ranges 219 to 248 mbsf, 300 to 333 mbsf, 400 to 500 mbsf, and 500 to 600 mbsf (Table 1, 2). The high felsic vein frequencies observed from 180-200 mbsf, 240-300 mbsf, 375-392 mbsf, and 580-620 mbsf did not correlate to higher cell abundances. The high carbonate vein frequencies observed from depths 248-274 mbsf, and 333-392 mbsf did not correlate to higher cell abundances. An explanation as to why cell concentrations are not higher in samples with high vein frequencies could be attributed to the scale at which the vein frequencies were observed. The vein frequencies were observed on a significantly larger scale, at every 10 m of core sample. The amount of rock sample use for cell counts is roughly 1 cm^3, which is significantly smaller in contrast to the 10 m core that were used to quantify vein frequencies. The presence of vein in the 10 m section, will not necessarily be present in the particular 1 cm^3 of rock sample that was used. In subsurface sedimentary environments, cell abundances typically decrease with respect to depth (Inagaki et al., 2015; Parkes et al., 1994), however, this is not the case for subsurface rock samples such as those featured in this experiment. Subsurface rock samples are heterogenous in nature and this heterogeneity translates into the cell abundances that have been enumerated along the core. Evidently, the cell counts do not decrease or increase with depth but rather remain consistently low in abundance and

adhere within the 10^2-10^3 cells/cm^3 range. Though care was taken to utilize the samples that had visible veins present for cell counts, the heterogenous nature of the rocks and discontinuous veins can account for the mismatch observed between vein frequencies and cell counts. In the same aforementioned study which enumerated cells at North Pond, the cell abundances showed a strong positive correlation to porosity, suggesting that microbial abundance in subsurface basalts can be controlled by geophysical or geochemical changes. However, the heterogenous nature of the samples present a challenge to study the effect of other parameters present *in situ* on the cell abundances (Zhang et al., 2016).

5.2 - Addressing Hypothesis 2: In situ microbial community structure and diversity is positively correlated to the number of veins.

5.2.1 – Correlation between Microbial Diversity and Vein Frequencies

While the most abundant class at each depth was variable, Nitrososphaeria, Alphaproteobacteria, and Gammaproteobacteria were abundant throughout all depths (Figure 4). The richness and diversity of the *in situ* samples varied greatly at different depths. Richness values were found to range from 4 to 219 ASVs per sample, and the diversity of the samples corresponded to the respective richness as well (Table 8). The most abundant genera at each depth were different at different depths (Table 7). In addition, the microbial diversity showed a very strong positive correlation to vein frequencies (Table 9). Higher vein frequencies suggest a larger surface area present within the rocks where microbes can travel to obtain nutrients, grow, and colonize. The very strong positive correlations suggest that higher vein frequencies are likely to facilitate microbial growth due to larger spatial availability.

5.2.2 - Interesting Genera Present in the In Situ Microbial Community

Samples from the *in situ* microbial communities present several interesting genera such as the Gammaproteobacterial SUP05 cluster was originally found in hydrothermal vent environments (Sunamura et al. 2004) and is also commonly found in the water column at the nitrite maxima of oxygen minimum zones (OMZ) (Shah et al., 2017).The SUP05 group plays a major role in the nitrogen cycling at vents and OMZs, where it couples sulfide oxidation to nitrate reduction (Hawley et al., 2014) helping to drive this fixed nitrogen loss (Callbeck et al., 2018). One notable genus that is abundant at 14 depths is Nitrospina, and this genus has the capability to oxidize nitrite; Nitrospina can also be found at OMZs in addition to surface waters (Luecker et al., 2013). Another interesting genus present is Candidatus Nitrosopelagicus, an archaeal genus that oxidizes ammonia and is typically found in the open ocean (Santoro et al., 2015). While each of these genera are abundant at different depths, at depths 404.9 mbsf, both Nitrospina and SUP05 are present, and at depth 247.7 mbsf, both Nitrospina and Candidatus Nitrosopelagicus are present. These genera are usually found in the marine water column, and it is possible that they were introduced into the lower oceanic crust by the circulation of seawater through the crust.

5.3 Addressing Hypothesis 3: Added nutrients will stimulate diversity in microbial communities.

5.3.1 - Nutrient Addition Treatment and Its Effects on Microbial Community Structure

The one-way ANOVA showed that the different treatments did not have a statistically significant effect on the microbial diversity of the incubation samples (Table 14). The response of the microbial community toward different treatments on the genus level was difficult to assess. For the majority of the incubations, genera that were highly abundant at a particular depth would typically be found in only one of the added treatments, but not in the incubation without any

treatments. This inconsistency in the presence of certain genera is most likely due to the heterogeneity of the rocks, meaning that the presence of microbial communities are likely dictated by the spatial availability in the rocks or mineralogy or other chemical and/or physical variation not detectable at the resolution of currently available methods. It could also be due to low microbial abundances in the samples or dead cells. In Figure 9, when dissimilarities were plotted on the ASV level in an NMDS plot, there was some clustering of bacterial communities with respect to the different treatments. One small clustering can be seen for the N-addition depths 420.9 and 639.3 mbsf, where both samples have an abundance of the genus Pelomonas. Several NP addition samples grouped together towards the center of the plot. The NP samples from depths 274.6 and 747.8 mbsf all had Hydrogenophilus as the most abundant genera, and for those from depths 626.3 and 639.3 mbsf, Altererythrobacter was one of the most abundant genus present in the samples. However, some larger similarity must be important for this grouping since there are also samples from all three other treatments in the grouping, and the genera mentioned above were not present in all the samples.

5.3.2 - Notable Genus from Incubation Samples

Hydrogenophilus was the most abundant genus found in the incubation samples, though it was only found in samples at depths 274.6, 460.4, 714.9, and 747.7 mbsf. The seven unique ASV's under *Hydrogenophilus* were identical at the nucleotide level to other *Hydrogenophilus* species commonly detected in geothermal environments (Arai et al., 2018; Hayashi et al., 1999; Vésteinsdóttir et al., 2011). *Hydrogenophilus* belongs to the Hydrogenophilalia class and Proteobacteria phylum (Boden et al., 2017). *H. thermoluteolus* and *H. hirschii,* the most studied isolates in this group, are moderately thermophilic and aerobic (Arai et al., 2018).

Hydrogenophilus are also facultative chemolithoautorophs that can grow autotrophically on hydrogen or sulfur compounds as the electron donor and carbon dioxide as the carbon source or heterotrophically in organic media. When growing autotrophically, *Hydrogenophilus* fixes carbon dioxide via the Calvin-Benson-Bassham (CBB) cycle (Arai et al., 2018).

5.3.3 - Similarities and Differences for Incubation and In situ Samples

The genera that the 40 samples have in common with the incubation samples include: *Aquabacterium*, *Bradyrhizobium*, *Brevundimonas*, *Clostridium*, *Curvibacter*, *Delftia*, *Formosa*, *Halomonas*, *Marinobacter*, *Methylobacterium*, *Pseudomonas*, *Pseudoxanthomonas*, *Rhizobium*, and *Stenotrophomonas*. Out of the 40 *in situ* samples, samples from nine depths were also used in the incubation experiments. From the nine samples in common with the incubation samples: the only shared genera are: *Rhizobium*, *Halomonas*, *Methylobacterium*, *Pseudomonas*, *Stenotrophomonas*.

The primary difference between the *in situ* and incubation samples is that archaeal genes were not amplifiable in the incubation samples. Methane was measured in the headspace of the incubation samples and it is postulated to be biotically produced because the methane produced in many of the vials were higher than that produced in the blank control, and also with just ASW and rocks, indicating the methane was likely formed via methanogenesis if it is assumed that the nutrients stimulated biological activity.. The abiotic formation of methane is a less likely source of the methane produced as this would have yielded similar amounts of methane for all samples. The lack of archaeal sequences from the DNA extraction do not necessarily point to an absence of Archaea. There have been reports of subsurface samples where multiple evidence pointed to the

presence of methanogenic Archaea, where none or only one archaeal 16S rRNA gene sequence was amplified; and archaeal 16S rRNA genes were not quantifiable by digital polymerase chain reaction (dPCR) either (Inagaki et al., 2015). In addition, major archaeal lineages are possibly not amplified due to sequence mismatches using domain-specific primers (Hoshino and Inagaki, 2019; Lipp et al., 2008; Teske and Sørensen, 2008), as were used here (and are commonly done). That said, the primers used here were specifically designed to more efficiently amplify common Archaea in seawater (Parada et al., 2016), so it is possible that the low recovery in the nutrient addition experiments is real.

Additionally, the community structure in the *in situ* and incubation samples differ vastly as can be seen by the difference in the dominant genera for the incubation and *in situ* samples at different depths. The nine *in situ* samples that were the original for the samples used in the nutrient addition incubation experiments can be used as time = 0, though between the *in situ* and incubation samples, only five shared genera were observed and within this genera, the ASVs were not similar. The differences in community could be attributed to changes within the community that occurred over the year long incubation. Moreover, another reason that could account for this dissimilarity is due to using different extraction methods; for the incubation samples, roughly 0.5 cm^3 of rocks were crushed using a sterile mortar and pestle prior to extracting DNA. The PCR polymerase enzyme used also differ for the differ between the *in situ* and incubation samples, as they were performed by different laboratories. The genera present in the *in situ* samples were most likely introduced from the marine water column, as mentioned above with genera such as Nitrospina and SUP05. In addition, the presence many of thermophilic bacteria in the incubation samples such as *Hydrogenophilus*, *Tepidimonas*, and *Anoxybacillus* could be indicative of these microbes being

introduced from much deeper depths, closer to the mantle where temperatures are significantly higher (Table 17).

5.4 - Addressing Hypothesis 4: Carbon additions, namely lactate, acetate and formate will enhance methane production.

Sampling of headspace after 25 and 60 weeks revealed the presence of methane in many incubations and the amounts were generally higher in incubations with added nutrients than in blank controls. The one-way ANOVA indicated that the different nutrient additions did not enhance methane production after 25 and 60 weeks. It was hypothesized that the addition of organic carbon sources, specifically lactate, acetate, and formate, would enhance methane production because these are common substrates that are used in acetoclastic methanogenesis. There are three major pathways of microbial methanogenesis: hydrogenotrophic, methylotrophic, and acetoclastic. Methylotrophic methanogenesis requires methylated compounds to produce methane (Lang et al., 2015), and an example of this is using methoxylated aromatic compounds produced within coal beds for methanogenesis (Mayumi et al., 2016). Hydrogenotrophic methanogenesis require H_2 and CO_2 to produce methane and is said to be the most widespread form of microbial methanogenesis as most methanogenic archaea can reduce CO_2 with H_2 to methane (Thauer et al., 2008). Though acetoclastic methanogenesis is responsible for biogenically produce methane in numerous environmental settings, only two genera from the order Methanosarcinales can utilize acetate to form methane (Ferry, 1992; Fournier and Gogarten, 2008; Stams et al., 2019). This could explain why the carbon addition samples did not show increased methane production. If there are methanogens present in the incubations, albeit undetected with 16S rRNA gene analysis, it is possible that the majority are not from the order Methanosarcinales,

and instead employ hydrogenotrophic methanogenesis. In which case, methane production could be positively linked to higher olivine content in the rocks, as H_2 is a product of serpentinization, from olivine reacting with water.

Another variable that the methane production was correlated to was vein frequency. More veins could allow for more interfaces between the rocks and seawater traveling through the veins. At these interfaces, microbes can benefit from the nutrient exchange, such as H_2 produced from serpentinization, which in turn can be positively correlated to higher methane production. There are high carbonate vein frequencies from depths 280 to 420 mbsf, and methane production after 60 weeks measured from depths 247.8, 274.6, 332.8, and 421.5 mbsf appear to be highest in productivity of methane. However, correlation coefficients for the relationship between methane production and vein frequency showed no correlation for methane produced up to 25 weeks, but a weak positive correlation for methane produced from 25-60 weeks. This indicates that vein frequencies might not be the factor that enhances methane production. If the methanogens present in the incubation are indeed utilizing hydrogenotrophic methanogenesis to produce methane, future work should include correlating the percent or weight of olivine mineral present at depths, or other lithological measurements such as vein thickness. While abiotic production of methane is said to be extremely limited in temperatures below 200°C due to kinetic inhibitions, there could be other explanations for the presence of methane that is not biogenically produced. such as the presence of volatiles released from fluid inclusions within the rocks, as well as thermal breakdown products of potential contaminant organic compounds in the rocks (McCollom, 2016).

5.5 - Additional Discussion: Role of Depth in Shaping the Microbial Community Structure

The general lithologies of the rock samples do not vary with depth and there is no postulated relationship between the lithology of the rocks and the microbial community structure. However, data from the incubation experiments showed that the most abundant genera for each depth differ distinctly. The closest known relatives for a majority of the sequences come from environments such as seawater from the Indian Ocean, soil, sediments and geothermal hot springs (Table 16). It is interesting to note that on the finer scale, e.g. between the rock samples from the same depth but in different nutrient additions, there is strong evidence of heterogeneity in the rocks that manifests as a specific genus found in one treatment, but not the others from the same depth. Despite this, the heterogeneity of the rocks appears to be less apparent on the larger scale, as can be seen from the different genera that are most abundant from the different depths.

6. CONCLUSION

Enumeration of cell abundances along the depth of the 790 m core allowed us to obtain an average of the microbial abundance present at this site. Assessment of the relationship between cell concentration and the presence and frequencies of veins helps to determine if evidence of fluid flow in the rocks affects the microbial population in terms of abundance. Vein presence was initially thought to have a positive correlation with cell concentration, as they are indicative of past fluid flow or fluid alterations, leaving behind pathways for microbial cells to move and obtain nutrients. Cell abundances throughout the length of the core remained low (10^2-10^3 cells/cm3). From depths 219-248, 300-333, and 400-600 mbsf, cell abundance showed a strong correlation to vein frequency. Other than these depth ranges, cell abundances did not follow a positive correlation to vein frequencies. This could be attributed to the heterogenous nature of the rocks, or how vein frequency was measured on a larger scale than the sample size used for cell counts. In order to assess if different nutrients play a role in shaping the microbial community structure, a nutrient addition incubation experiment was set up using rock samples from 12 selected depths along the core. It was hypothesized that nutrient addition would promote higher diversity in microbial communities. Single-factor ANOVA proved that each nutrient treatment did not have a statistically different effect on the microbial diversity. Upon analyzing the microbial community based on depth, there was a clear difference in the dominant genera present for each depth. NMDS plots depicted a few genera that clustered together based on nutrient additions, such as *Hydrogenophilus* and *Altererythrobacter* in the NP additions, and *Pelomonas* in the C-additions. Additionally, no archaeal sequences were amplified from the incubation samples despite methane being measured in the headspace of the incubation vials. It was also hypothesized that methane production in the incubation samples would increase with the carbon addition would correlate positively to vein

presence. However, there was no statistically significant difference in the effect of the different treatments or vein frequencies on methane production. Future work to better understand what regulates the microbial abundance and microbial community in subsurface rock environments include correlations with other lithological or geochemical properties of the rocks such as oxide composition, in addition to metagenomic analyses of several promising samples such as those from depths with higher abundance and highest diversity in sequences. The analysis performed here provided insight to understanding the microbial life at an ultraslow spreading ridge in the Indian Ocean, and allow for a better understanding of lower oceanic crust microbiology as well.

REFERENCES

Arai, H., Shomura, Y., Yoshiki, H., Ishii, M., 2018. Complete Genome Sequence of a Moderately Thermophilic Facultative Chemolithoautotrophic Hydrogen-Oxidizing Bacterium, Hydrogenophilus thermoluteolus TH-1 | Microbiology Resource Announcements.

Biddle, J.F., Fitz-Gibbon, S., Schuster, S.C., Brenchley, J.E., House, C.H., 2008. Metagenomic signatures of the Peru Margin subseafloor biosphere show a genetically distinct environment. Proc. Natl. Acad. Sci. U.S.A. 105, 10583–10588. https://doi.org/10.1073/pnas.0709942105

Blackman, D.K., Ildefonse, B., John, B.E., Ohara, Y., Miller, D.J., Abe, N., Abratis, M., Andal, E.S., Andreani, M., Awaji, S., Beard, J.S., Brunelli, D., Charney, A.B., Christie, D.M., Collins, J.A., Delacour, A.G., Delius, H., Drouin, M., Einaudi, F., Escartin, J.E., Frost, B.R., Fruh-Green, G.L., Fryer, P.B., Gee, J.S., Grimes, C.B., Halfpenny, A., Hansen, H.-E., Harris, A.C., Tamura, A., Hayman, N.W., Hellebrand, E., Hirose, T., Hirth, G., Ishimaru, S., Johnson, K.T.M., Karner, G.D., Linek, M., MacLeod, C.J., Maeda, J., Mason, O.U., McCaig, A.M., Michibayashi, K., Morris, A., Nakagawa, T., Nozaka, T., Rosner, M., Searle, R.C., Suhr, G., Tominaga, M., von der Handt, A., Yamasaki, T., Zhao, X., 2011. Drilling constraints on lithospheric accretion and evolution at Atlantis Massif, Mid-Atlantic Ridge 30°N. Journal of Geophysical Research-Solid Earth. https://doi.org/10.1029/2010JB007931

Blackman, D.K., Ildefonse, B., Ohara, Y., Miller, D.J., MacLeod, C., J., Expedition 304/305 Scientists, 2006. Proceedings, IODP, 304/305. Integrated Ocean Drilling Program Management International, Inc. https://doi.org/doi:10.2204/iodp.proc.304305.103.2006

Boden, R., Hutt, L.P., Rae, A.W., 2017. Reclassification of Thiobacillus aquaesulis (Wood & Kelly, 1995) as Annwoodia aquaesulis gen. nov., comb. nov., transfer of Thiobacillus (Beijerinck, 1904) from the Hydrogenophilales to the Nitrosomonadales, proposal of Hydrogenophilalia class. nov. within the 'Proteobacteria', and four new families within the orders Nitrosomonadales and Rhodocyclales. International Journal of Systematic and Evolutionary Microbiology 67, 1191–1205. https://doi.org/10.1099/ijsem.0.001927

Brazelton, W.J., Mehta, M.P., Kelley, D.S., Baross, J.A., 2011. Physiological differentiation within a single-species biofilm fueled by serpentinization. MBio 2. https://doi.org/10.1128/mBio.00127-11

Brazelton, W.J., Nelson, B., Schrenk, M.O., 2012. Metagenomic Evidence for H2 Oxidation and H2 Production by Serpentinite-Hosted Subsurface Microbial Communities. Front Microbiol 2. https://doi.org/10.3389/fmicb.2011.00268

Brazelton, W.J., Schrenk, M.O., Kelley, D.S., Baross, J.A., 2006. Methane- and Sulfur-Metabolizing Microbial Communities Dominate the Lost City Hydrothermal Field Ecosystem. Appl Environ Microbiol 72, 6257–6270. https://doi.org/10.1128/AEM.00574-06

Callahan, B.J., McMurdie, P.J., Holmes, S.P., 2017. Exact sequence variants should replace operational taxonomic units in marker-gene data analysis. The ISME Journal 11, 2639–2643. https://doi.org/10.1038/ismej.2017.119

Callahan, B.J., McMurdie, P.J., Rosen, M.J., Han, A.W., Johnson, A.J.A., Holmes, S.P., 2016. DADA2: High-resolution sample inference from Illumina amplicon data. Nature Methods 13, 581–583. https://doi.org/10.1038/nmeth.3869

Callbeck, C.M., Lavik, G., Ferdelman, T.G., Fuchs, B., Gruber-Vodicka, H.R., Hach, P.F., Littmann, S., Schoffelen, N.J., Kalvelage, T., Thomsen, S., Schunck, H., Löscher, C.R., Schmitz, R.A., Kuypers, M.M.M., 2018. Oxygen minimum zone cryptic sulfur cycling sustained by offshore transport of key sulfur oxidizing bacteria. Nature Communications 9, 1729. https://doi.org/10.1038/s41467-018-04041-x

Cannat, M., Sauter, D., Mendel, V., Ruellan, E., Okino, K., Escartin, J., Combier, V., Baala, M., 2006. Modes of seafloor generation at a melt-poor ultraslow-spreading ridge. {GEOLOGY} {34}. https://doi.org/{10.1130/G22486.1}

Caporaso, J.G., Lauber, C.L., Walters, W.A., Berg-Lyons, D., Huntley, J., Fierer, N., Owens, S.M., Betley, J., Fraser, L., Bauer, M., Gormley, N., Gilbert, J.A., Smith, G., Knight, R., 2012. Ultra-high-throughput microbial community analysis on the Illumina HiSeq and MiSeq platforms. ISME J 6, 1621–1624. https://doi.org/10.1038/ismej.2012.8

Chen, S., Shao, Z., 2008. Isolation and diversity analysis of arsenite-resistant bacteria in communities enriched from deep-sea sediments of the Southwest Indian Ocean Ridge. Extremophiles 13, 39–48. https://doi.org/10.1007/s00792-008-0195-1

Chen, W.-M., Huang, H.-W., Chang, J.-S., Han, Y.-L., Guo, T.-R., Sheu, S.-Y., 2013. Tepidimonas fonticaldi sp. nov., a slightly thermophilic betaproteobacterium isolated from a hot spring. Int. J. Syst. Evol. Microbiol. 63, 1810–1816. https://doi.org/10.1099/ijs.0.043729-0

Choi, J.-H., Kim, M.-S., Roh, S.W., Bae, J.-W., 2010. Acidovorax soli sp. nov., isolated from landfill soil. Int. J. Syst. Evol. Microbiol. 60, 2715–2718. https://doi.org/10.1099/ijs.0.019661-0

Claesson, M.J., Wang, Q., O'Sullivan, O., Greene-Diniz, R., Cole, J.R., Ross, R.P., O'Toole, P.W., 2010. Comparison of two next-generation sequencing technologies for resolving highly complex microbiota composition using tandem variable 16S rRNA gene regions. Nucleic Acids Res. 38, e200. https://doi.org/10.1093/nar/gkq873

Coorevits, A., Dinsdale, A.E., Halket, G., Lebbe, L., De Vos, P., Van Landschoot, A., Logan, N.A., 2012. Taxonomic revision of the genus Geobacillus: emendation of Geobacillus, G. stearothermophilus, G. jurassicus, G. toebii, G. thermodenitrificans and G. thermoglucosidans (nom. corrig., formerly 'thermoglucosidasius'); transfer of Bacillus thermantarcticus to the genus as G. thermantarcticus comb. nov.; proposal of Caldibacillus debilis gen. nov., comb. nov.; transfer of G. tepidamans to Anoxybacillus as A. tepidamans comb. nov.; and proposal of Anoxybacillus caldiproteolyticus sp. nov. Int. J. Syst. Evol. Microbiol. 62, 1470–1485. https://doi.org/10.1099/ijs.0.030346-0

Cowen, J.P., Giovannoni, S.J., Kenig, F., Johnson, H.P., Butterfield, D., Rappé, M.S., Hutnak, M., Lam, P., 2003. Fluids from Aging Ocean Crust That Support Microbial Life. Science 299, 120–123. https://doi.org/10.1126/science.1075653

Dick, H.J.B., Lin, J., Schouten, H., 2003. An ultraslow-spreading class of ocean ridge. Nature 426, 405–412. https://doi.org/10.1038/nature02128

Dick, H.J.B., MacLeod, C., J., Blum, P., Expedition 360 Scientists, 2016. Proceedings of the International Ocean Discovery Program Volume 360 Expedition Reports. https://doi.org/10.14379/iodp.proc.360.2017

Ding, J., Zhang, Y., Wang, H., Jian, H., Leng, H., Xiao, X., 2017. Microbial Community Structure of Deep-sea Hydrothermal Vents on the Ultraslow Spreading Southwest Indian Ridge. Front Microbiol 8, 1012. https://doi.org/10.3389/fmicb.2017.01012

Ding, L., Yokota, A., 2004. Proposals of Curvibacter gracilis gen. nov., sp. nov. and Herbaspirillum putei sp. nov. for bacterial strains isolated from well water and reclassification of [Pseudomonas] huttiensis, [Pseudomonas] lanceolata, [Aquaspirillum] delicatum and [Aquaspirillum] autotrophicum as Herbaspirillum huttiense comb. nov., Curvibacter lanceolatus comb. nov., Curvibacter delicatus comb. nov. and Herbaspirillum autotrophicum comb. nov. Int. J. Syst. Evol. Microbiol. 54, 2223–2230. https://doi.org/10.1099/ijs.0.02975-0

Ferry, J.G., 1992. Methane from acetate. Journal of Bacteriology 174, 5489–5495. https://doi.org/10.1128/jb.174.17.5489-5495.1992

Fournier, G.P., Gogarten, J.P., 2008. Evolution of Acetoclastic Methanogenesis in Methanosarcina via Horizontal Gene Transfer from Cellulolytic Clostridia. Journal of Bacteriology 190, 1124–1127. https://doi.org/10.1128/JB.01382-07

Früh-Green, G.L., Orcutt, B.N., Rouméjon, S., Lilley, M.D., Morono, Y., Cotterill, C., Green, S., Escartin, J., John, B.E., McCaig, A.M., Cannat, M., Ménez, B., Schwarzenbach, E.M., Williams, M.J., Morgan, S., Lang, S.Q., Schrenk, M.O., Brazelton, W.J., Akizawa, N., Boschi, C., Dunkel, K.G., Quéméneur, M., Whattam, S.A., Mayhew, L., Harris, M., Bayrakci, G., Behrmann, J.H., Herrero-Bervera, E., Hesse, K., Liu, H.Q., Ratnayake, A.S., Twing, K., Weis, D., Zhao, R., Bilenker, L., 2018. Magmatism, serpentinization and life: Insights through drilling the Atlantis Massif (IODP Expedition 357). LITHOS 323, 137–155. https://doi.org/10.1016/j.lithos.2018.09.012

Gößner, A.S., Devereux, R., Ohnemüller, N., Acker, G., Stackebrandt, E., Drake, H.L., 1999. Thermicanus aegyptius gen. nov., sp. nov., Isolated from Oxic Soil, a Fermentative Microaerophile That Grows Commensally with the Thermophilic Acetogen Moorella thermoacetica. Appl Environ Microbiol 65, 5124–5133.

Guo, B., Liu, Y., Gu, Z., Shen, L., Liu, K., Wang, N., Xing, T., Liu, H., Zhou, Y., Li, J., 2016. Massilia psychrophila sp. nov., isolated from an ice core. Int. J. Syst. Evol. Microbiol. 66, 4088–4093. https://doi.org/10.1099/ijsem.0.001315

Hawley, A.K., Brewer, H.M., Norbeck, A.D., Paša-Tolić, L., Hallam, S.J., 2014. Metaproteomics reveals differential modes of metabolic coupling among ubiquitous oxygen minimum zone microbes. PNAS 111, 11395–11400. https://doi.org/10.1073/pnas.1322132111

Hayashi, N.R., Ishida, T., Yokota, A., Kodama, T., Igarashi, Y., 1999. Hydrogenophilus thermoluteolus gen. nov., sp. nov., a thermophilic, facultatively chemolithoautotrophic, hydrogen-oxidizing bacterium. Int. J. Syst. Bacteriol. 49 Pt 2, 783–786. https://doi.org/10.1099/00207713-49-2-783

Heberling, C., Lowell, R.P., Liu, L., Fisk, M.R., 2010. Extent of the microbial biosphere in the oceanic crust. Geochemistry, Geophysics, Geosystems 11, Q08003. https://doi.org/10.1029/2009GC002968

Hoshino, T., Inagaki, F., 2019. Abundance and distribution of Archaea in the subseafloor sedimentary biosphere. The ISME Journal 13, 227. https://doi.org/10.1038/s41396-018-0253-3

Huang, H.-Y., Chen, Y.-G., Wang, Y.-X., Liu, J.-H., Tang, S.-K., Peng, Q., Wen, M.-L., Yu, H., Cui, X.-L., 2008. Halomonas sediminis sp. nov., a new halophilic bacterium isolated

from salt-lake sediment in China. Extremophiles 12, 829–835. https://doi.org/10.1007/s00792-008-0189-z

Inagaki, F., Hinrichs, K.-U., Kubo, Y., Bowles, M.W., Heuer, V.B., Hong, W.-L., Hoshino, T., Ijiri, A., Imachi, H., Ito, M., Kaneko, M., Lever, M.A., Lin, Y.-S., Methé, B.A., Morita, S., Morono, Y., Tanikawa, W., Bihan, M., Bowden, S.A., Elvert, M., Glombitza, C., Gross, D., Harrington, G.J., Hori, T., Li, K., Limmer, D., Liu, C.-H., Murayama, M., Ohkouchi, N., Ono, S., Park, Y.-S., Phillips, S.C., Prieto-Mollar, X., Purkey, M., Riedinger, N., Sanada, Y., Sauvage, J., Snyder, G., Susilawati, R., Takano, Y., Tasumi, E., Terada, T., Tomaru, H., Trembath-Reichert, E., Wang, D.T., Yamada, Y., 2015. Exploring deep microbial life in coal-bearing sediment down to ~2.5 km below the ocean floor. Science 349, 420–424. https://doi.org/10.1126/science.aaa6882

Inagaki, F., Nunoura, T., Nakagawa, S., Teske, A., Lever, M., Lauer, A., Suzuki, M., Takai, K., Delwiche, M., Colwell, F.S., Nealson, K.H., Horikoshi, K., D'Hondt, S., Jørgensen, B.B., 2006. Biogeographical distribution and diversity of microbes in methane hydrate-bearing deep marine sediments on the Pacific Ocean Margin. PNAS 103, 2815–2820. https://doi.org/10.1073/pnas.0511033103

Johnson, K., M., Hughes, J., E., Donaghay, P., L., Sieburth, J., M., 1990. Bottle-calibration static head space method for the determination of methane dissolved in seawater.

Jørgensen, N.O.G., Brandt, K.K., Nybroe, O., Hansen, M., 2009. Delftia lacustris sp. nov., a peptidoglycan-degrading bacterium from fresh water, and emended description of Delftia tsuruhatensis as a peptidoglycan-degrading bacterium. Int. J. Syst. Evol. Microbiol. 59, 2195–2199. https://doi.org/10.1099/ijs.0.008375-0

Jørgensen, Zhao, R., 2016. Microbial Inventory of Deeply Buried Oceanic Crust from a Young Ridge Flank. Front Microbiol 7, 820. https://doi.org/10.3389/fmicb.2016.00820

Jungbluth, S.P., Grote, J., Lin, H.-T., Cowen, J.P., Rappé, M.S., 2013. Microbial diversity within basement fluids of the sediment-buried Juan de Fuca Ridge flank. ISME J 7, 161–172. https://doi.org/10.1038/ismej.2012.73

Kallmeyer, J., Pockalny, R., Adhikari, R.R., Smith, D.C., D'Hondt, S., 2012. Global distribution of microbial abundance and biomass in subseafloor sediment. PNAS 109, 16213–16216. https://doi.org/10.1073/pnas.1203849109

Kelley, D.S., Karson, J.A., Blackman, D.K., Früh-Green, G.L., Butterfield, D.A., Lilley, M.D., Olson, E.J., Schrenk, M.O., Roe, K.K., Lebon, G.T., Rivizzigno, P., AT3-60 Shipboard Party, 2001. An off-axis hydrothermal vent field near the Mid-Atlantic Ridge at 30 degrees N. Nature 412, 145–149. https://doi.org/10.1038/35084000

Kelley, D.S., Karson, J.A., Früh-Green, G.L., Yoerger, D.R., Shank, T.M., Butterfield, D.A., Hayes, J.M., Schrenk, M.O., Olson, E.J., Proskurowski, G., Jakuba, M., Bradley, A., Larson, B., Ludwig, K., Glickson, D., Buckman, K., Bradley, A.S., Brazelton, W.J., Roe, K., Elend, M.J., Delacour, A., Bernasconi, S.M., Lilley, M.D., Baross, J.A., Summons, R.E., Sylva, S.P., 2005. A Serpentinite-Hosted Ecosystem: The Lost City Hydrothermal Field. Science 307, 1428–1434. https://doi.org/10.1126/science.1102556

Kröncke, I., Tan, T.L., Stein, R., 1994. High benthic bacteria standing stock in deep Arctic basins | SpringerLink.

Kwon, T., Baek, K., Lee, K., Kang, I., Cho, J.-C., 2014. Formosa arctica sp. nov., isolated from Arctic seawater. Int. J. Syst. Evol. Microbiol. 64, 78–82. https://doi.org/10.1099/ijs.0.056465-0

Lai, Q., Yuan, J., Shao, Z., 2009. Altererythrobacter marinus sp. nov., isolated from deep seawater. Int. J. Syst. Evol. Microbiol. 59, 2973–2976. https://doi.org/10.1099/ijs.0.008193-0

Lang, K., Schuldes, J., Klingl, A., Poehlein, A., Daniel, R., Brune, A., 2015. New Mode of Energy Metabolism in the Seventh Order of Methanogens as Revealed by Comparative Genome Analysis of "Candidatus Methanoplasma termitum." Appl Environ Microbiol 81, 1338–1352. https://doi.org/10.1128/AEM.03389-14

Lever, M.A., Alperin, M., Engelen, B., Inagaki, F., Nakagawa, S., Steinsbu, B.O., Teske, A., 2006. Trends in Basalt and Sediment Core Contamination During IODP Expedition 301: Geomicrobiology Journal: Vol 23, No 7.

Lever, M.A., Rouxel, O., Alt, J.C., Shimizu, N., Ono, S., Coggon, R.M., Shanks, W.C., Lapham, L., Elvert, M., Prieto-Mollar, X., Hinrichs, K.-U., Inagaki, F., Teske, A., 2013. Evidence for Microbial Carbon and Sulfur Cycling in Deeply Buried Ridge Flank Basalt. Science 339, 1305–1308. https://doi.org/10.1126/science.1229240

Li, Jiwei, Peng, X., Zhou, H., Li, Jiangtao, Sun, Z., 2013. Molecular evidence for microorganisms participating in Fe, Mn, and S biogeochemical cycling in two low-temperature hydrothermal fields at the Southwest Indian Ridge. Journal of Geophysical Research (Biogeosciences) 118, 665–679. https://doi.org/10.1002/jgrg.20057

Lipp, J.S., Morono, Y., Inagaki, F., Hinrichs, K.-U., 2008. Significant contribution of Archaea to extant biomass in marine subsurface sediments. Nature 454, 991–994. https://doi.org/10.1038/nature07174

Luecker, S., Nowka, B., Rattei, T., Spieck, E., Daims, H., 2013. The Genome of Nitrospina gracilis Illuminates the Metabolism and Evolution of the Major Marine Nitrite Oxidizer. Front. Microbiol. 4. https://doi.org/10.3389/fmicb.2013.00027

MacLeod, C., J., Dick, H.J.B., Blum, P., Abe, N., Blackman, D., K., Bowles, J., A., Cheadle, M., J., Cho, K., Ciążela, J., Deans, J.R., Edgcomb, V.P., Ferrando, C., France, L., Ghosh, B., Ildefonse, B., M., Kendrick, M.A., Koepke, J.H., Leong, J.A.M., Liu, C., Ma, Q., Morishita, T., Morris, A., Natland, J.H., Nozaka, T., Pluemper, O., Sanfilippo, A., Sylvan, J.B., Tivey, M.A., Tribuzio, R., Viegas, L.G.F., 2017. Expedition 360 Methods. Proceedings of the International Ocean Discovery Program. https://doi.org/10.14379/iodp.proc.360.102.2017

Martin, W., Baross, J.A., Kelley, D.S., Russell, M.J., 2008. Hydrothermal vents and the origin of life | Nature Reviews Microbiology.

Mason, O.U., Nakagawa, T., Rosner, M., Van Nostrand, J.D., Zhou, J., Maruyama, A., Fisk, M.R., Giovannoni, S.J., 2010. First Investigation of the Microbiology of the Deepest Layer of Ocean Crust. PLoS One 5. https://doi.org/10.1371/journal.pone.0015399

Mayumi, D., Mochimaru, H., Tamaki, H., Yamamoto, K., Yoshioka, H., Suzuki, Y., Kamagata, Y., Sakata, S., 2016. Methane production from coal by a single methanogen. Science 354, 222–225. https://doi.org/10.1126/science.aaf8821

McCollom, T.M., 2016. Abiotic methane formation during experimental serpentinization of olivine. PNAS 113, 13965–13970. https://doi.org/10.1073/pnas.1611843113

McMurdie, P.J., Holmes, S., 2013. phyloseq: An R Package for Reproducible Interactive Analysis and Graphics of Microbiome Census Data. PLoS ONE.

Meyer, J.L., Jaekel, U., Tully, B.J., Glazer, B.T., Wheat, C.G., Lin, H.-T., Hsieh, C.-C., Cowen, J.P., Hulme, S.M., Girguis, P.R., Huber, J.A., 2016. A distinct and active bacterial community in cold oxygenated fluids circulating beneath the western flank of the Mid-Atlantic ridge. Scientific Reports. https://doi.org/10.1038/srep22541

Michael, P.J., Langmuir, C.H., Dick, H.J.B., Snow, J.E., Goldstein, S.L., Graham, D.W., Lehnert, K., Kurras, G., Jokat, W., Mühe, R., Edmonds, H.N., 2003. Magmatic and amagmatic seafloor generation at the ultraslow-spreading Gakkel ridge, Arctic Ocean. Nature 423, 956–961. https://doi.org/10.1038/nature01704

Morono, Y., Terada, T., Kallmeyer, J., Inagaki, F., 2013. An improved cell separation technique for marine subsurface sediments: applications for high-throughput analysis using flow cytometry and cell sorting. Environ. Microbiol. 15, 2841–2849. https://doi.org/10.1111/1462-2920.12153

Nemec, A., Radolfova-Krizova, L., Maixnerova, M., Vrestiakova, E., Jezek, P., Sedo, O., 2016. Taxonomy of haemolytic and/or proteolytic strains of the genus Acinetobacter with the proposal of Acinetobacter courvalinii sp. nov. (genomic species 14 sensu Bouvet & Jeanjean), Acinetobacter dispersus sp. nov. (genomic species 17), Acinetobacter modestus sp. nov., Acinetobacter proteolyticus sp. nov. and Acinetobacter vivianii sp. nov. Int. J. Syst. Evol. Microbiol. 66, 1673–1685. https://doi.org/10.1099/ijsem.0.000932

Oksanen, J., Blanchet, F.G., Friendly, M., Kindt, R., Legendre, P., McGlinn, D., Minchin, P.R., O'Hara, R.B., Simpson, G.L., Solymos, P., H. Stevens, M.H., Szoecs, E., Wagner, H., 2019. vegan: Community Ecology Package version 2.5-5 from CRAN.

Orcutt, B.N., Wheat, C.G., Rouxel, O., Hulme, S., Edwards, K.J., Bach, W., 2013. Oxygen consumption rates in subseafloor basaltic crust derived from a reaction transport model. Nature Communications 4, 2539. https://doi.org/10.1038/ncomms3539

Orsi, W.D., Edgcomb, V.P., Christman, G.D., Biddle, J.F., 2013. Gene expression in the deep biosphere. Nature 499, 205–208. https://doi.org/10.1038/nature12230

Parada, A.E., Needham, D.M., Fuhrman, J.A., 2016. Every base matters: assessing small subunit rRNA primers for marine microbiomes with mock communities, time series and global field samples. Environ. Microbiol. 18, 1403–1414. https://doi.org/10.1111/1462-2920.13023

Parkes, R.J., Cragg, B.A., Bale, S.J., Getlifff, J.M., Goodman, K., Rochelle, P.A., Fry, J.C., Weightman, A.J., Harvey, S.M., 1994. Deep bacterial biosphere in Pacific Ocean sediments. Nature 371, 410–413. http://dx.doi.org/10.1038/371410a0

Pham, V.H.T., Jeong, S., Chung, S., Kim, J., 2016. Brevundimonas albigilva sp. nov., isolated from forest soil. Int. J. Syst. Evol. Microbiol. 66, 1144–1150. https://doi.org/10.1099/ijsem.0.000848

Rosen, M.J., Callahan, B.J., Fisher, D.S., Holmes, S.P., 2012. Denoising PCR-amplified metagenome data. BMC Bioinformatics 13, 283. https://doi.org/10.1186/1471-2105-13-283

Ruiz-García, C., Béjar, V., Martínez-Checa, F., Llamas, I., Quesada, E., 2005. Bacillus velezensis sp. nov., a surfactant-producing bacterium isolated from the river Vélez in Málaga, southern Spain. Int. J. Syst. Evol. Microbiol. 55, 191–195. https://doi.org/10.1099/ijs.0.63310-0

Saitoh, S., Suzuki, T., Nishimura, Y., 1998. Proposal of Craurococcus roseus gen. nov., sp. nov. and Paracraurococcus ruber gen. nov., sp. nov., novel aerobic bacteriochlorophyll a-containing bacteria from soil. Int. J. Syst. Bacteriol. 48 Pt 3, 1043–1047. https://doi.org/10.1099/00207713-48-3-1043

Salter, S.J., Cox, M.J., Turek, E.M., Calus, S.T., Cookson, W.O., Moffatt, M.F., Turner, P., Parkhill, J., Loman, N.J., Walker, A.W., 2014. Reagent and laboratory contamination can critically impact sequence-based microbiome analyses. BMC Biology 12, 87. https://doi.org/10.1186/s12915-014-0087-z

Santoro, A.E., Dupont, C.L., Richter, R.A., Craig, M.T., Carini, P., McIlvin, M.R., Yang, Y., Orsi, W.D., Moran, D.M., Saito, M.A., 2015. Genomic and proteomic characterization of "Candidatus Nitrosopelagicus brevis": an ammonia-oxidizing archaeon from the open ocean. Proc. Natl. Acad. Sci. U.S.A. 112, 1173–1178. https://doi.org/10.1073/pnas.1416223112

Schäffer, C., Franck, W.L., Scheberl, A., Kosma, P., McDermott, T.R., Messner, P., 2004. Classification of isolates from locations in Austria and Yellowstone National Park as Geobacillus tepidamans sp. nov. Int. J. Syst. Evol. Microbiol. 54, 2361–2368. https://doi.org/10.1099/ijs.0.63227-0

Schloss, P.D., Westcott, S.L., Ryabin, T., Hall, J.R., Hartmann, M., Hollister, E.B., Lesniewski, R.A., Oakley, B.B., Parks, D.H., Robinson, C.J., Sahl, J.W., Stres, B., Thallinger, G.G., Horn, D.J.V., Weber, C.F., 2009. Introducing mothur: Open-Source, Platform-Independent, Community-Supported Software for Describing and Comparing Microbial Communities. Appl. Environ. Microbiol. 75, 7537–7541. https://doi.org/10.1128/AEM.01541-09

Schrenk, M.O., Brazelton, W.J., Lang, S.Q., 2013. Serpentinization , Carbon , and Deep Life - Semantic Scholar.

Schrenk, M.O., Kelley, D.S., Bolton, S.A., Baross, J.A., 2004. Low archaeal diversity linked to subseafloor geochemical processes at the Lost City Hydrothermal Field, Mid-Atlantic Ridge. Environ. Microbiol. 6, 1086–1095. https://doi.org/10.1111/j.1462-2920.2004.00650.x

Shah, V., Chang, B.X., Morris, R.M., 2017. Cultivation of a chemoautotroph from the SUP05 clade of marine bacteria that produces nitrite and consumes ammonium | The ISME Journal. The ISME Journal 11, 263–271.

Sheik, C.S., Reese, B.K., Twing, K.I., Sylvan, J.B., Grim, S.L., Schrenk, M.O., Sogin, M.L., Colwell, F.S., 2018. Identification and Removal of Contaminant Sequences From Ribosomal Gene Databases: Lessons From the Census of Deep Life. Front. Microbiol. 9. https://doi.org/10.3389/fmicb.2018.00840

Shen, L., Liu, Y., Gu, Z., Xu, B., Wang, N., Jiao, N., Liu, H., Zhou, Y., 2015. Massilia eurypsychrophila sp. nov. a facultatively psychrophilic bacteria isolated from ice core. Int. J. Syst. Evol. Microbiol. 65, 2124–2129. https://doi.org/10.1099/ijs.0.000229

Shih, P.M., Wu, D., Latifi, A., Axen, S.D., Fewer, D.P., Talla, E., Calteau, A., Cai, F., Tandeau de Marsac, N., Rippka, R., Herdman, M., Sivonen, K., Coursin, T., Laurent, T., Goodwin, L., Nolan, M., Davenport, K.W., Han, C.S., Rubin, E.M., Eisen, J.A., Woyke, T., Gugger, M., Kerfeld, C.A., 2013. Improving the coverage of the cyanobacterial phylum using diversity-driven genome sequencing. Proc. Natl. Acad. Sci. U.S.A. 110, 1053–1058. https://doi.org/10.1073/pnas.1217107110

Smith, A., Popa, R., Fisk, M., Nielsen, M., Wheat, C.G., Jannasch, H.W., Fisher, A.T., Becker, K., Sievert, S.M., Flores, G., 2011. In situ enrichment of ocean crust microbes on igneous minerals and glasses using an osmotic flow-through device. Geochemistry, Geophysics, Geosystems 12, Q06007. https://doi.org/10.1029/2010GC003424

Smith, M.R., 1999. Stone: Building Stone, Rock Fill and Armourstone in Construction. Geological Society of London.

Stams, A.J.M., Teusink, B., Souza, D.Z., 2019. Ecophysiology of Acetoclastic Methanogens, in: Biogenesis of Hydrocarbons. pp. 1–14.

Subhash, Y., Tushar, L., Sasikala, C., Ramana, C.V., 2013. Falsirhodobacter halotolerans gen. nov., sp. nov., isolated from dry soils of a solar saltern. Int. J. Syst. Evol. Microbiol. 63, 2132–2137. https://doi.org/10.1099/ijs.0.044107-0

Sylvan, J.B., Hoffman, C.L., Momper, L.M., Toner, B.M., Amend, J.P., Edwards, K.J., 2015. Bacillus rigiliprofundi sp. nov., an endospore-forming, Mn-oxidizing, moderately halophilic bacterium isolated from deep subseafloor basaltic crust. Int. J. Syst. Evol. Microbiol. 65, 1992–1998. https://doi.org/10.1099/ijs.0.000211

Takai, K., Gamo, T., Tsunogai, U., Nakayama, N., Hirayama, H., Nealson, K.H., Horikoshi, K., 2004. Geochemical and microbiological evidence for a hydrogen-based, hyperthermophilic subsurface lithoautotrophic microbial ecosystem (HyperSLiME) beneath an active deep-sea hydrothermal field. Extremophiles 8, 269–282. https://doi.org/10.1007/s00792-004-0386-3

Tazato, N., Handa, Y., Nishijima, M., Kigawa, R., Sano, C., Sugiyama, J., 2015. Novel environmental species isolated from the plaster wall surface of mural paintings in the Takamatsuzuka tumulus: Bordetella muralis sp. nov., Bordetella tumulicola sp. nov. and

Bordetella tumbae sp. nov. Int. J. Syst. Evol. Microbiol. 65, 4830–4838. https://doi.org/10.1099/ijsem.0.000655

Teske, A., Sørensen, K.B., 2008. Uncultured archaea in deep marine subsurface sediments: have we caught them all? ISME J 2, 3–18. https://doi.org/10.1038/ismej.2007.90

Thauer, R.K., Kaster, A.-K., Seedorf, H., Buckel, W., Hedderich, R., 2008. Methanogenic archaea: ecologically relevant differences in energy conservation. Nat. Rev. Microbiol. 6, 579–591. https://doi.org/10.1038/nrmicro1931

Tiago, I., Mendes, V., Pires, C., Morais, P.V., Verśsimo, A., 2005. Phenylobacterium falsum sp. nov., an Alphaproteobacterium isolated from a nonsaline alkaline groundwater, and emended description of the genus Phenylobacterium. Syst. Appl. Microbiol. 28, 295–302.

Valentine, D.L., Kessler, J.D., Redmond, M.C., Mendes, S.D., Heintz, M.B., Farwell, C., Hu, L., Kinnaman, F.S., Yvon-Lewis, S., Du, M., Chan, E.W., Garcia Tigreros, F., Villanueva, C.J., 2010. Propane respiration jump-starts microbial response to a deep oil spill. Science 330, 208–211. https://doi.org/10.1126/science.1196830

Vésteinsdóttir, H., Reynisdóttir, D.B., Orlygsson, J., 2011. Hydrogenophilus islandicus sp. nov., a thermophilic hydrogen-oxidizing bacterium isolated from an Icelandic hot spring. Int. J. Syst. Evol. Microbiol. 61, 290–294. https://doi.org/10.1099/ijs.0.023572-0

Walters, W., Hyde, E.R., Berg-Lyons, D., Ackermann, G., Humphrey, G., Parada, A., Gilbert, J.A., Jansson, J.K., Caporaso, J.G., Fuhrman, J.A., Apprill, A., Knight, R., 2016. Improved Bacterial 16S rRNA Gene (V4 and V4-5) and Fungal Internal Transcribed Spacer Marker Gene Primers for Microbial Community Surveys. mSystems 1. https://doi.org/10.1128/mSystems.00009-15

Wang, E.T., van Berkum, P., Sui, X.H., Beyene, D., Chen, W.X., Martínez-Romero, E., 1999. Diversity of rhizobia associated with Amorpha fruticosa isolated from Chinese soils and description of Mesorhizobium amorphae sp. nov. Int. J. Syst. Bacteriol. 49 Pt 1, 51–65. https://doi.org/10.1099/00207713-49-1-51

Whitman, W.B., Coleman, D.C., Wiebe, W.J., 1998. Prokaryotes: The unseen majority. PNAS 95, 6578–6583. https://doi.org/10.1073/pnas.95.12.6578

Xie, C.-H., Yokota, A., 2005. Reclassification of Alcaligenes latus strains IAM 12599T and IAM 12664 and Pseudomonas saccharophila as Azohydromonas lata gen. nov., comb. nov., Azohydromonas australica sp. nov. and Pelomonas saccharophila gen. nov., comb. nov., respectively. Int. J. Syst. Evol. Microbiol. 55, 2419–2425. https://doi.org/10.1099/ijs.0.63733-0

Yao, L., Zhang, J.-J., Yu, L.-L., Chen, Q., Zhu, J.-C., He, J., Ding, D.-R., 2016. Rhizorhabdus dicambivorans sp. nov., a dicamba-degrading bacterium isolated from compost. Int. J. Syst. Evol. Microbiol. 66, 3317–3323. https://doi.org/10.1099/ijsem.0.001194

Zhang, X., Feng, X., Wang, F., 2016. Diversity and Metabolic Potentials of Subsurface Crustal Microorganisms from the Western Flank of the Mid-Atlantic Ridge. Front Microbiol 7. https://doi.org/10.3389/fmicb.2016.00363

APPENDIX A: FIGURES

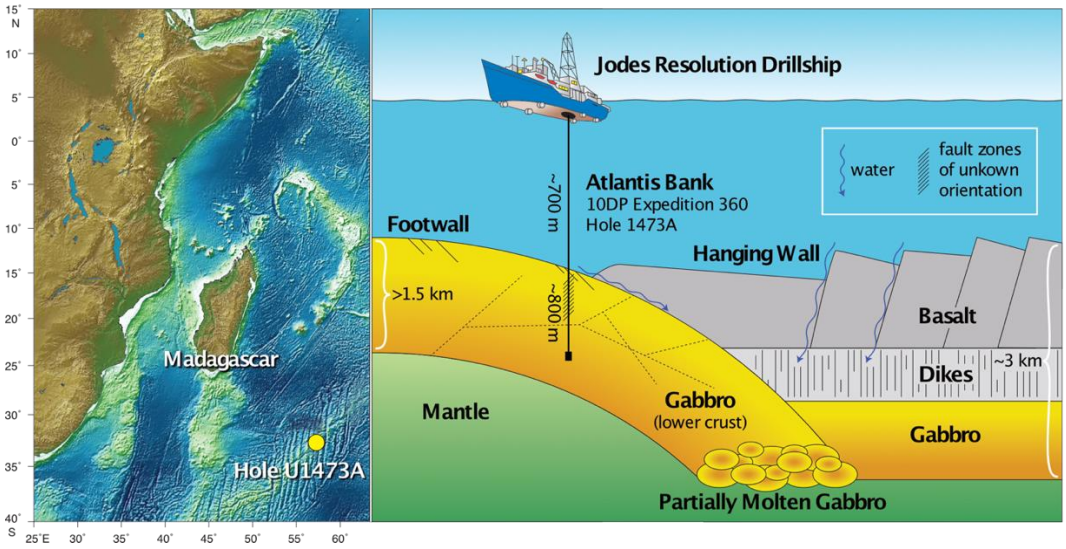

Figure 1. Study site for IODP Expedition 360 exploration of the intrusive oceanic crust.

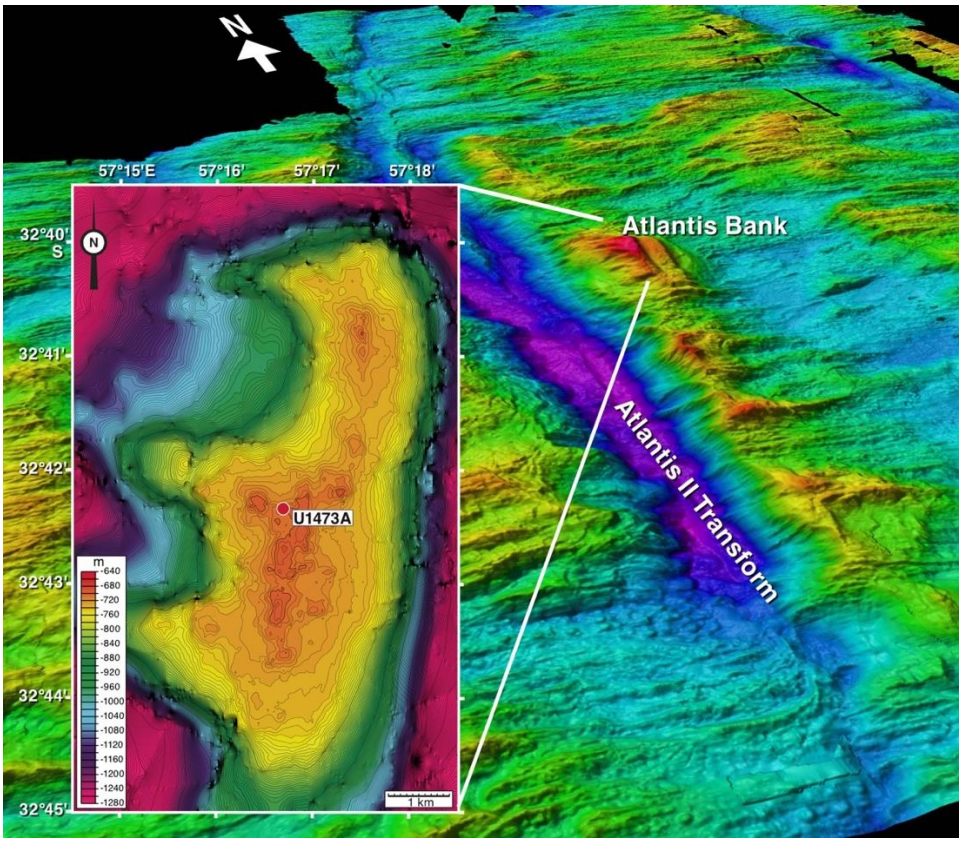

Figure 2. Site map for Atlantis Bank and exact location of Hole U1473A. Reprinted from Proceedings of the International Ocean Discovery Program Volume 360 Expedition Reports (Dick et al., 2016).

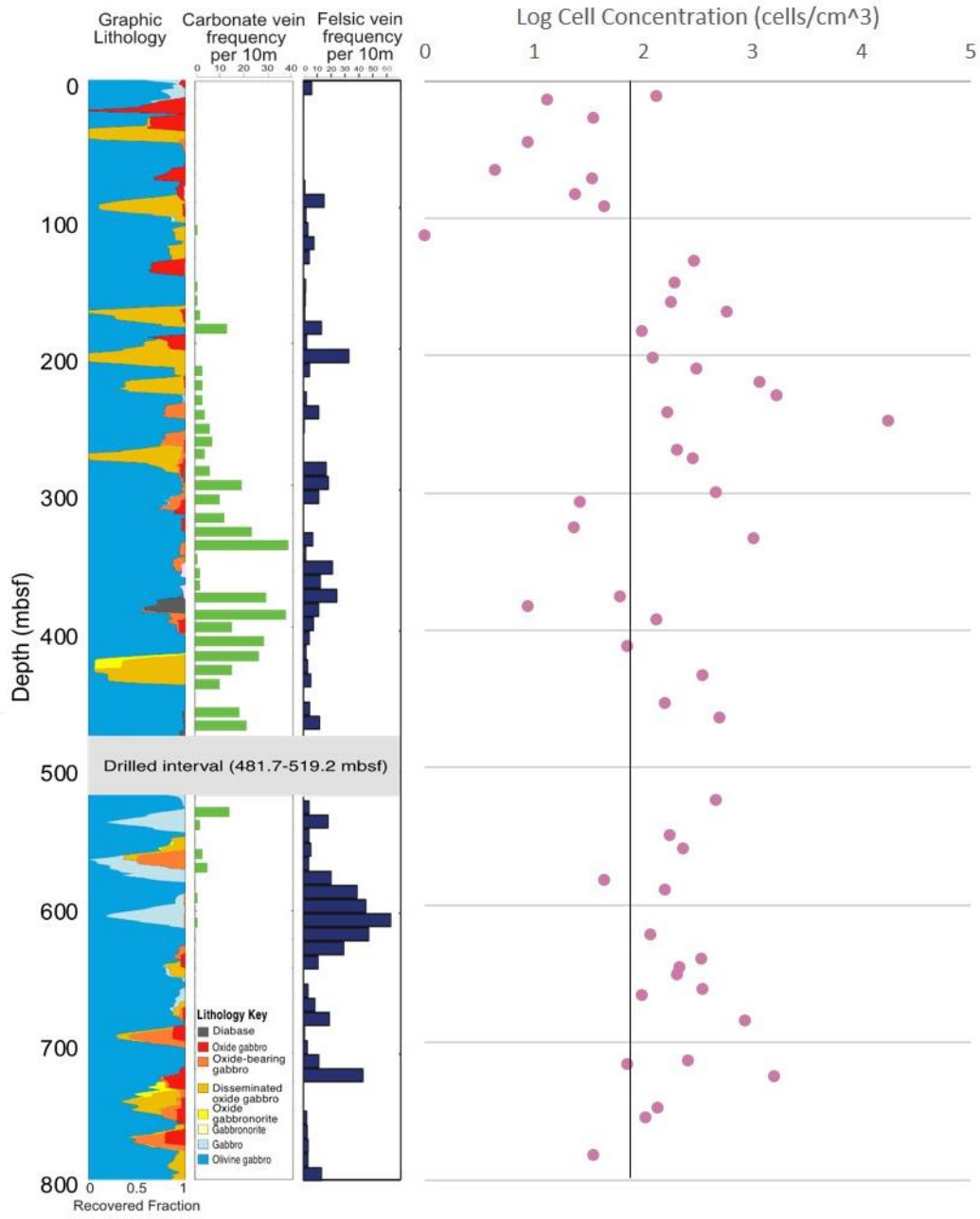

Figure 3. Plot of cell abundance against core depth, in addition to carbonate vein and felsic vein frequency, and the lithology present on the core at each depth. The black line refers to limit of quantification.

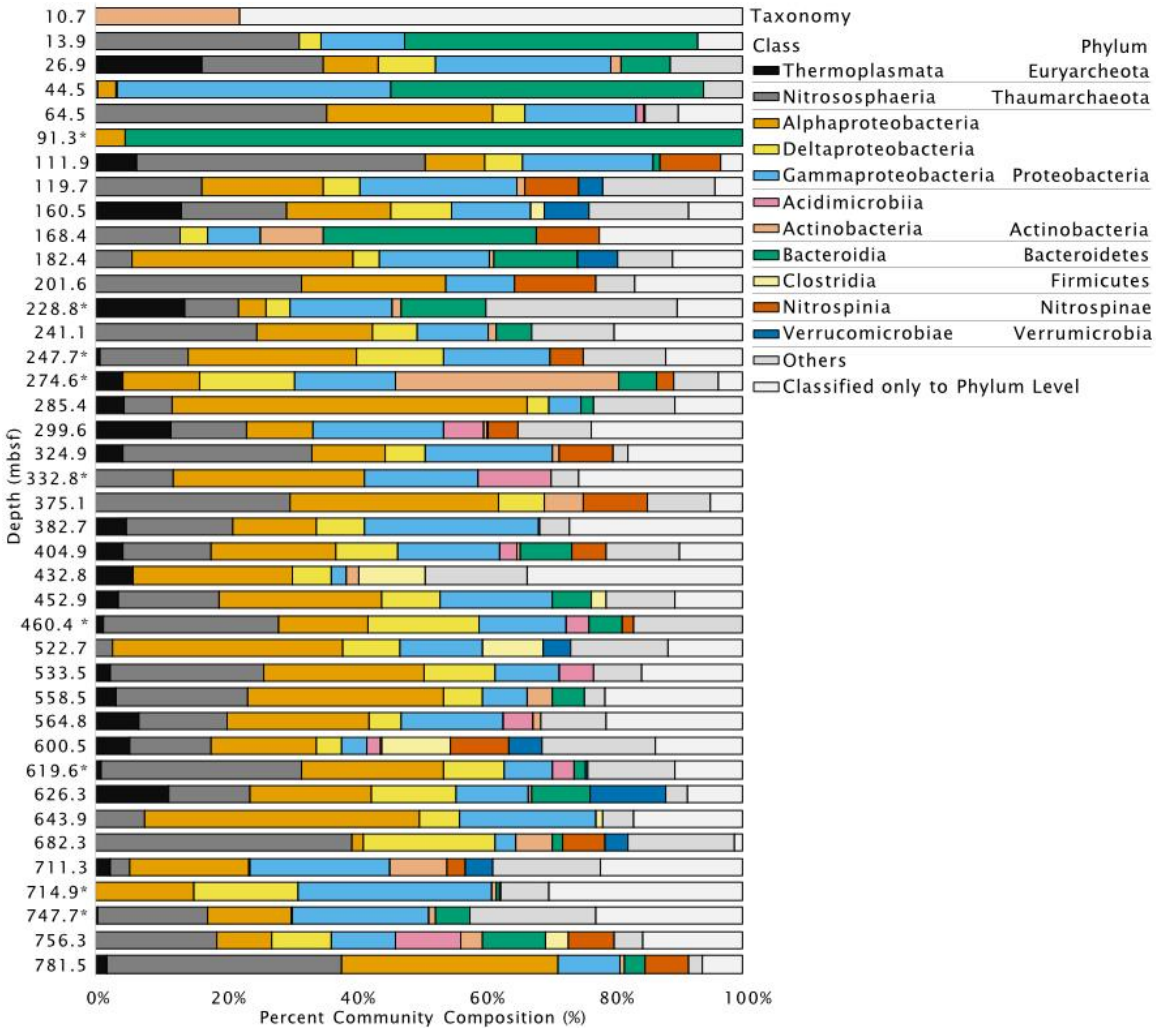

Figure 4. Microbial community composition for the 40 *in situ* rock samples at the Class taxonomic level. The Phylum level is also annotated in the legend for each Class. *Asterisks mark samples from depths that are also present in the incubation experiments.

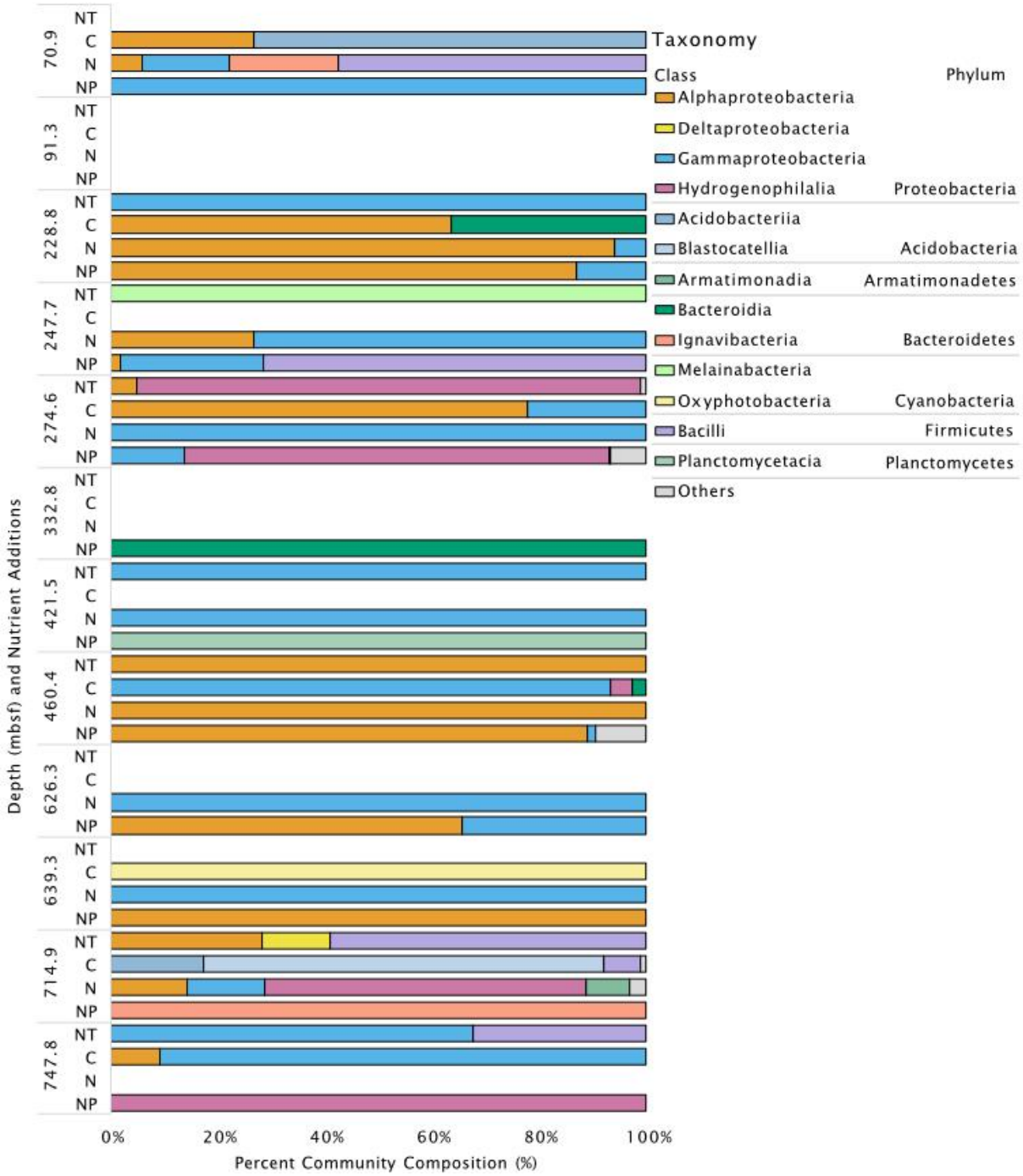

Figure 5. Microbial community composition for nutrient addition incubation experiments presented at the class taxonomic level. NT: No treatment, C: Carbon (lactate, acetate and formate) addition, N: Ammonium addition, NP: Ammonium and phosphate addition.

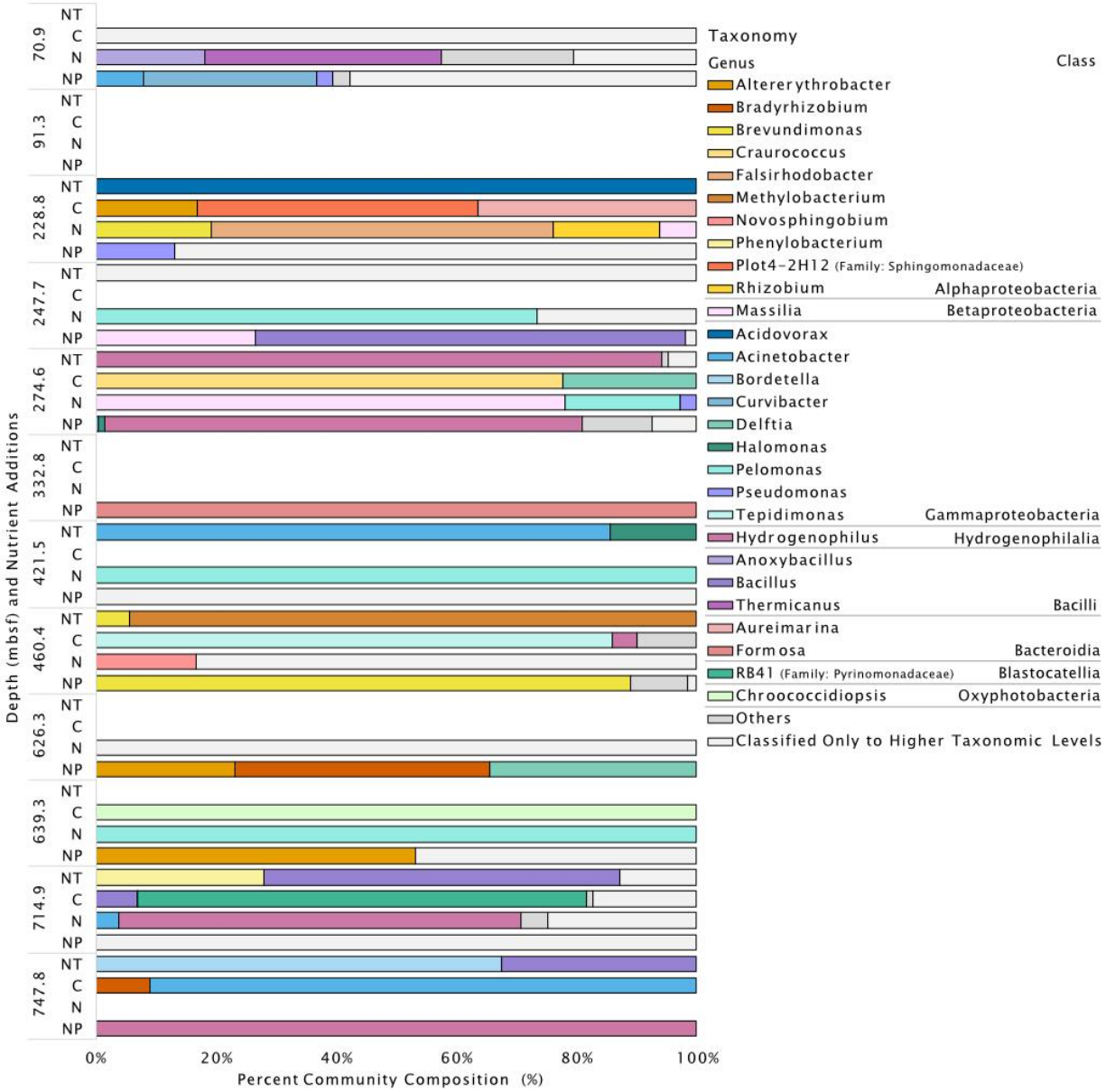

Figure 6. Microbial community composition for nutrient addition incubation experiments presented on the genus taxonomic level. NT: No treatment, C: Carbon (lactate, acetate and formate) addition, N: Ammonium addition, NP: Ammonium and phosphate addition.

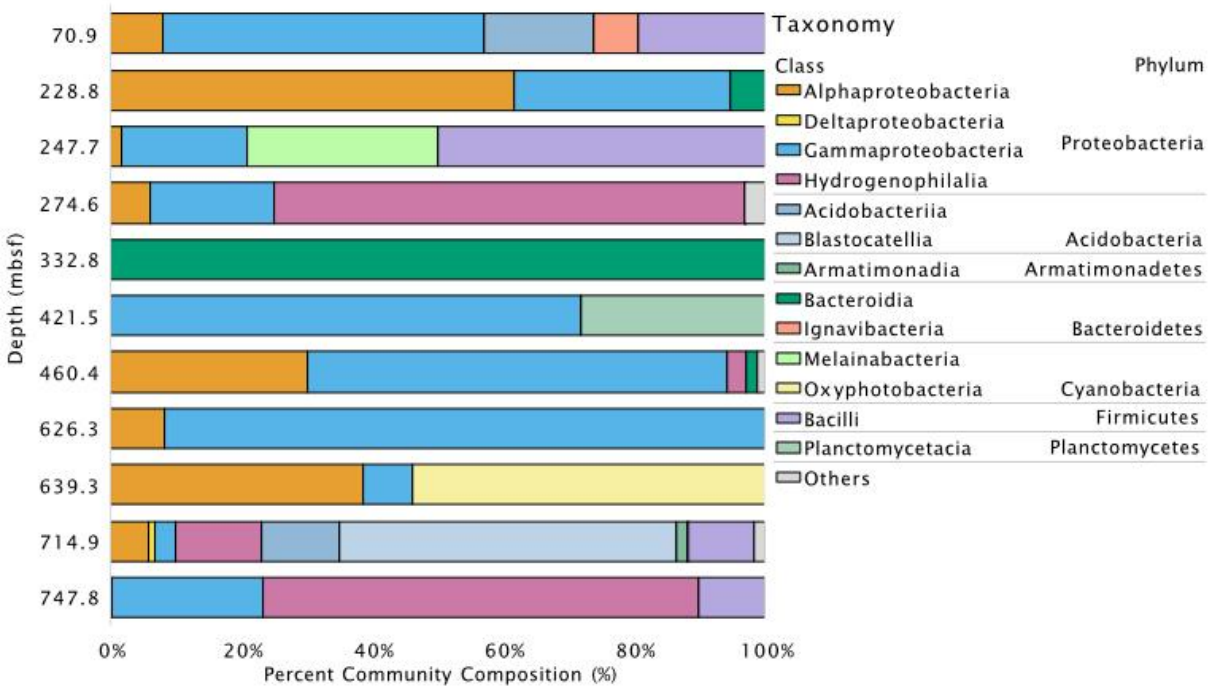

Figure 7. Microbial community composition at the class taxonomic level for all the combined samples from the nutrient addition incubation experiments, grouped into their respective depths.

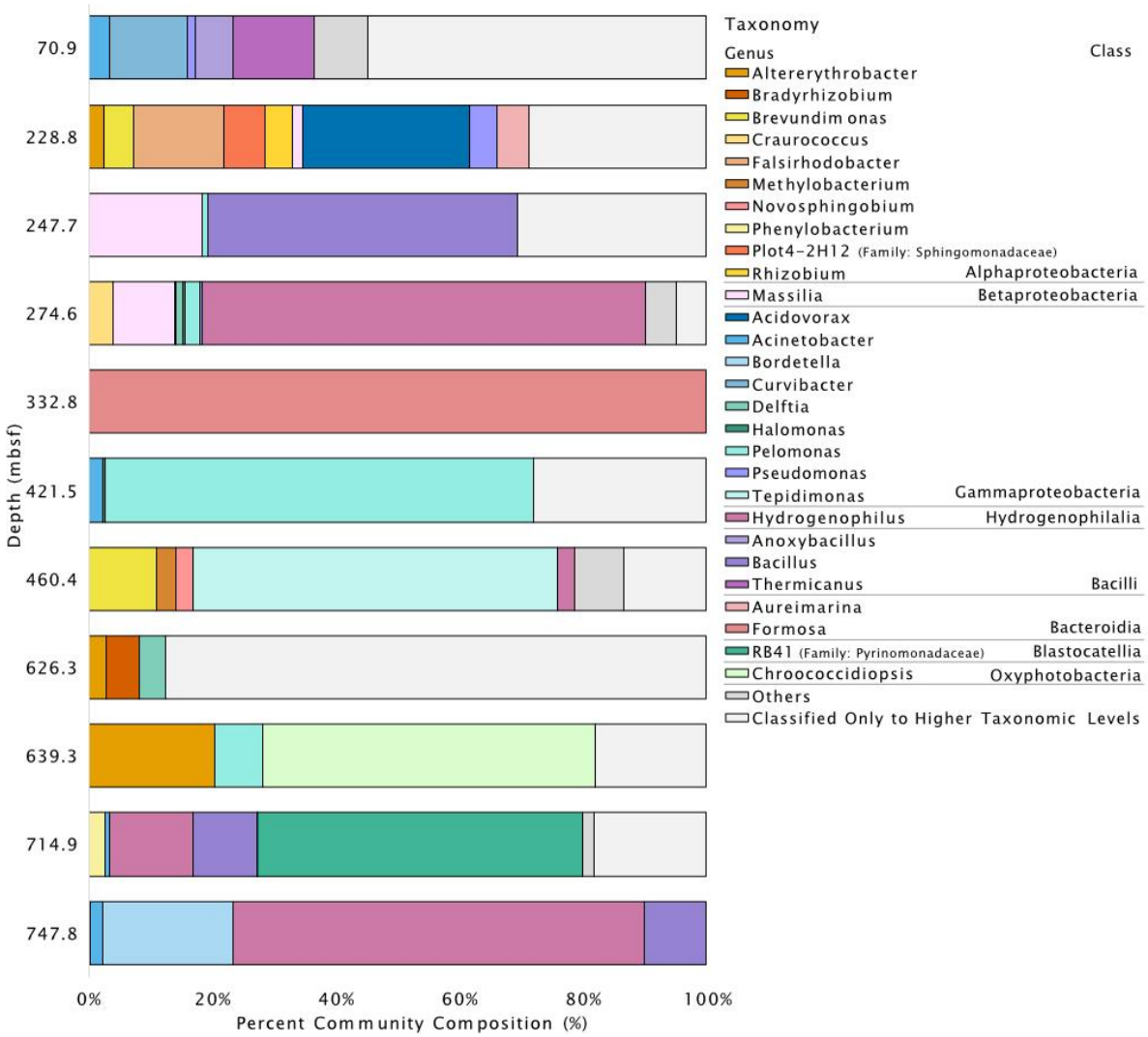

Figure 8. Microbial community composition on the genus taxonomic level for all the combined samples from the nutrient addition incubation experiments, grouped into their respective depths.

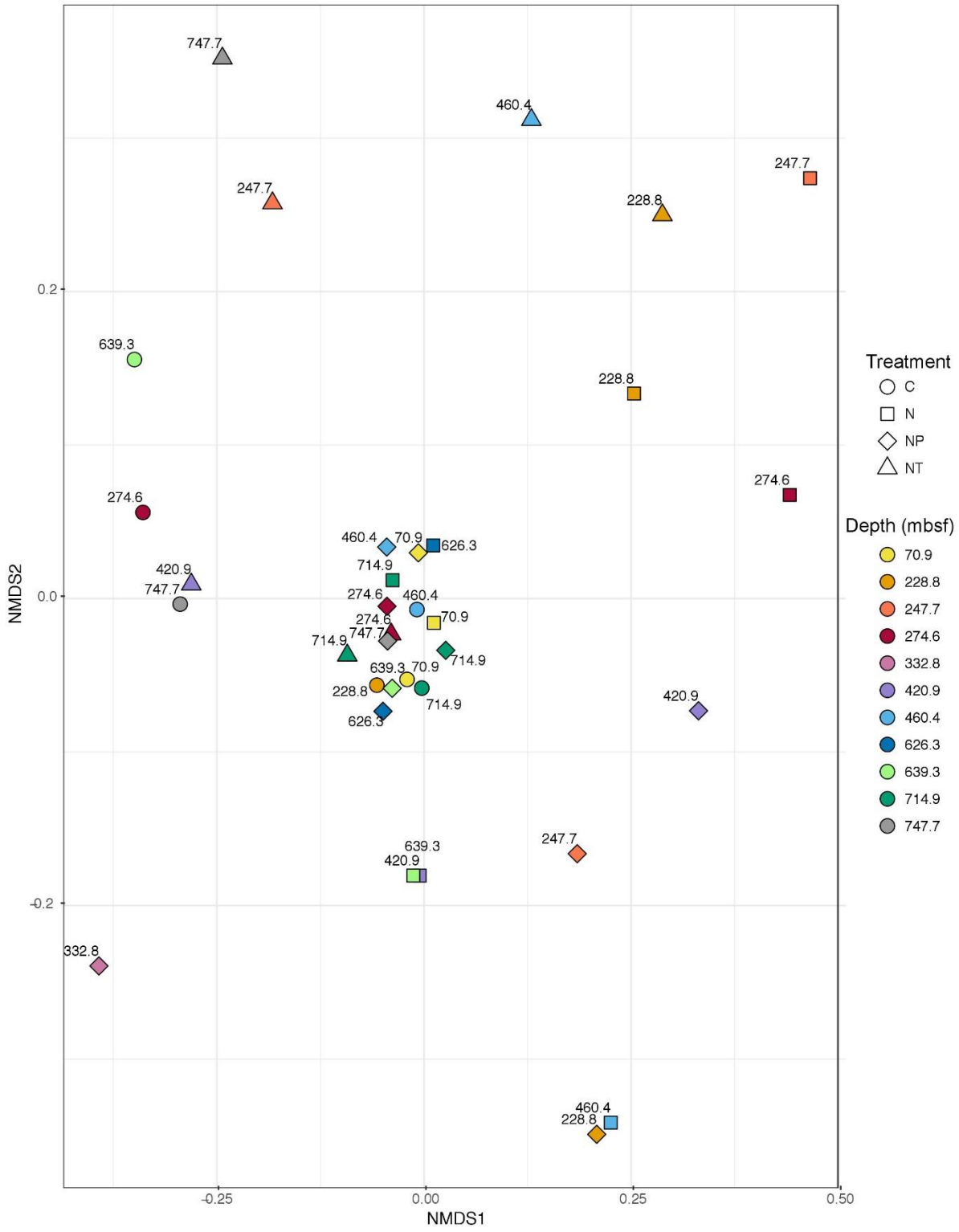

Figure 9. NMDS plot of dissimilarity in microbial community for each nutrient addition incubation sample. Each color corresponds to a different depth and each shape corresponds to a different treatment. Labels for depth are also added for ease of visualization. The stress value for the NMDS plot is 0.000120.

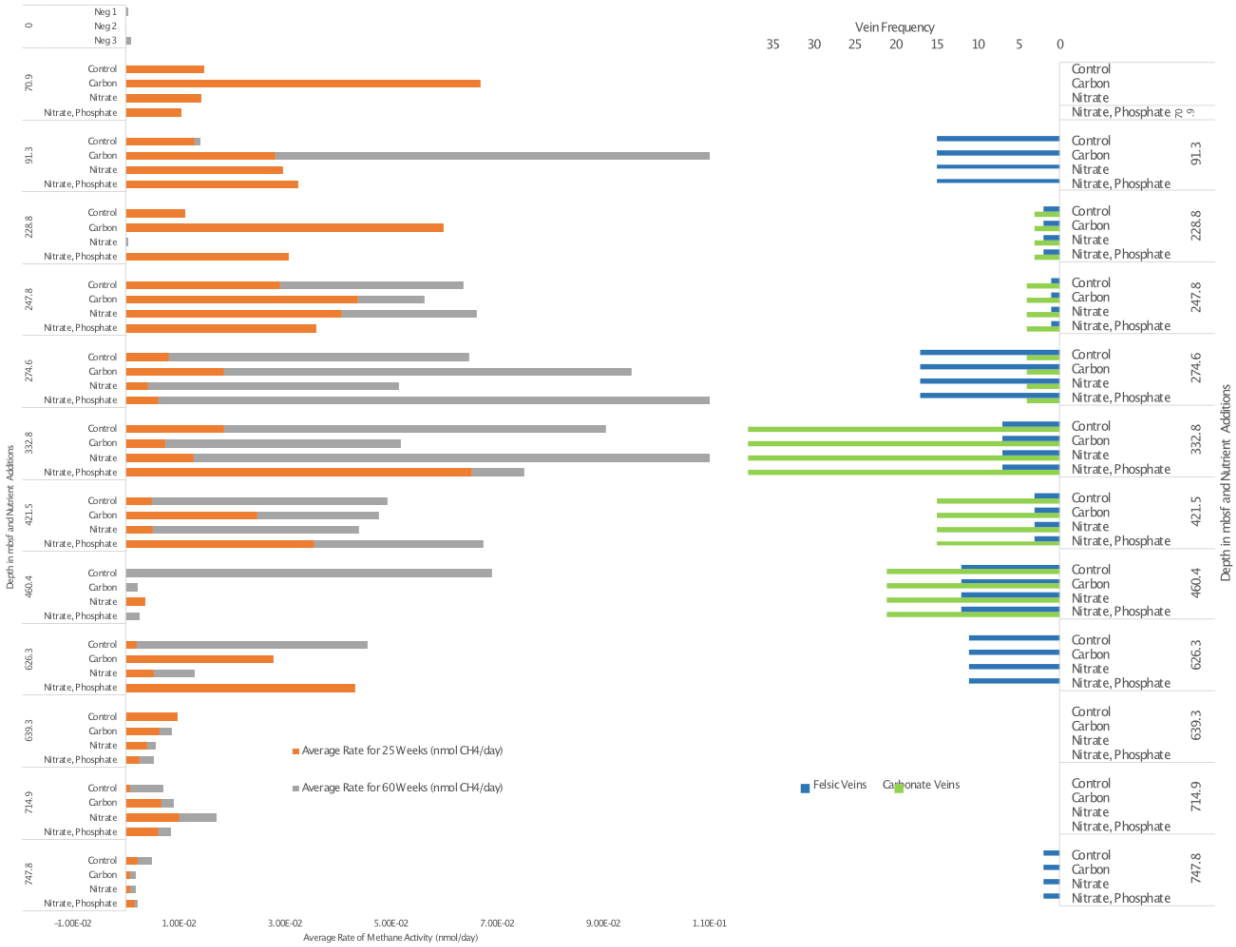

Figure 10. Rate of methane production in long term enrichment experiments (left). The carbonate and felsic vein frequency present in the 10 m core transect is shown for reference (right).

APPENDIX B: TABLES

Table 1. Recipe for artificial seawater (ASW).

Component	Amount/Concentration
18.2 MΩ·cm Milli-Q water	1000 mL/L
NaCl	27.5 g/L
$MgCl_2 \cdot 6H_2O$	8.8 g/L
KCl	0.5 g/L
Na_2SO_4	3.3 g/L
Na_2CO_3	25 mM
$CaCl_2 \cdot 2H_2O$	1.4 g/L
$(NH_4)_2SO_4$	0.63 g/L
$K_2HPO_4 \cdot 3H_2O$	0.04 g/L
KBr	0.05 g/L
H_3BO_3	0.02 g/L
ATCC-TMS	10 mL/L
Resazurin	1 mg/L
Sodium thioglycolate	2 g/L
Sigma Kao & Michayluk Vitamins Solution	10 mL/L
Thioctin (α-lipoic) acid	500 mg
1x ATCC Trace Mineral Supplement	10 mL/L

Table 2. Correlation coefficients for cell abundance and vein frequency in rock samples for depth ranges of every 100 meters below seafloor.

Depth Range (mbsf)	Pearson Correlation Coefficient, Pe	
	Carbonate Vein Frequency	Felsic Vein Frequency
0-100	NA	0.431
100-200	-0.237	-0.349
200-300	-0.055	-0.318
300-400	0.501	-0.049
400-500	-0.398	0.922
500-600	0.830	-0.645
600-700	-0.185	-0.221
700-800	NA	-0.200
All Depths	-0.024	-0.111

Legend	Description
Pe = 1	Perfect positive correlation
0.75 ≤ Pe < 1	Very strong positive correlation
0.50 ≤ Pe < 0.75	Moderate positive correlation
0.25 ≤ Pe < 0.5	Weak positive correlation
0 < Pe < 0.25	Negligible correlation
Pe = 0	No correlation
-0.25 < Pe < 0	Negligible correlation
-0.50 < Pe ≤ -0.25	Weak negative correlation
-0.75 ≤ Pe ≤ -0.5	Moderate negative correlation
-0.75 ≤ Pe < -1	Very strong negative correlation
Pe = -1	Perfect negative correlation

Table 3. Correlation coefficients for cell abundance and vein frequency in rock samples for varying depth ranges, selected based on depths where either cell abundances or vein frequencies were highest.

Reasoning for Depth Range Selection	Depth Range (mbsf)	Pearson Correlation Coefficient, Pe		Cell Counts Data Points
		Carbonate Vein Frequency	Felsic Vein Frequency	
High cell counts	218-247	0.997	-0.391	4
High felsic vein frequency	241-299	-0.273	-0.534	5
High carbonate vein frequency	247-274	-0.504	-0.450	3
High cell counts	299-332	0.842	0.683	4
High carbonate vein frequency	299-392	0.420	-0.019	7
High carbonate vein frequency	332-392	0.427	-0.454	4
High felsic vein frequency	375-392	-0.997	-0.289	3
High carbonate vein frequency	411-463	-0.398	0.922	4
High cell counts	432-463	0.195	0.887	3
High felsic vein frequency	581-621	-0.842	0.234	3
High cell counts	639-724	-0.184	-0.173	9
High felsic vein frequency	661-781	0.000	-0.191	9

Table 4. Number of ASVs and reads constructed with the initial *in situ* 16S rRNA data for each sample, followed by the numbers remaining after removal of ASVs present in the blank PCR control, and numbers remaining after quality control (removal of ASVs that are commonly found in PCR contamination).

Depth (mbsf)	Initial		Removal of Blank Controls		Removal of Common PCR Contaminants	
	# of ASV	# of Reads	# of ASV	# of Reads	# of ASV	# of Reads
10.7	51	88999	23	293	4	27
13.9	53	76589	22	10247	8	86
26.9	132	5375	42	1786	28	1384
44.5	113	160870	50	4552	20	3547
64.5	323	35562	145	10468	107	8938
91.3	55	52956	51	52734	6	348
111.9	71	82337	33	500	11	173
119.7	368	27306	188	8244	142	5888
160.5	250	7894	106	3344	51	2110
168.4	85	96545	33	447	12	122
182.4	565	57470	357	35175	232	15353
201.6	463	46041	243	15398	127	11671
209	58	95609	17	11867	0	0
228.8	316	34706	160	7740	124	6717
241.1	406	40231	205	13172	136	8824
247.7	313	213520	153	6910	56	1866
274.6	370	458416	216	10127	40	1384
285.4	136	3543	51	1900	43	1829
299.6	331	25271	186	7502	108	4577
306.7	68	105421	32	460	0	0
324.9	232	8676	89	2275	74	2008
332.8	128	36602	65	27990	17	308
375.1	77	34553	61	34171	13	183
382.7	237	12248	88	2908	76	2500
404.9	537	57511	346	19051	193	11940
420.9	5	207	4	99	0	0
432.8	219	11615	109	4356	79	3363
452.9	390	31878	189	8780	152	7692
460.4	383	42737	217	21934	111	8396
522.7	227	68465	101	66272	29	1326
533.5	108	165277	74	163861	23	862
558.5	225	9711	111	4783	87	3043
564.8	387	74856	193	15950	123	12192
600.5	458	90396	254	23560	180	19754

Table 4 continued

Depth (mbsf)	Initial		Removal of Blank Controls		Removal of Common PCR Contaminants	
	# of ASV	# of Reads	# of ASV	# of Reads	# of ASV	# of Reads
619.6	470	105551	262	34943	175	28517
626.3	133	70405	54	6550	21	606
643.9	170	4729	76	2755	34	1335
682.3	265	10182	104	3620	67	2199
711.3	384	21237	200	8009	167	6705
714.9	257	44620	96	5719	53	3428
747.7	487	76190	277	42793	98	6152
756.3	179	4340	60	1765	45	1522
781.5	227	7338	79	2122	63	1924
Blank Kit Control	456	56776	0	0	0	0
PCR Control	348	68692	0	0	0	0
Total	5,202*	2,829,453	4,541* (87.3% of initial)	707,132	2,649* (50.9% of initial)	200,701

*Total ASVs are the number of every unique ASV present for all samples, it is not the cumulative number of ASVs from each depth and treatment.

Table 5. Community composition of all *in situ* samples on the phylum level for Bacteria and Archaea.

Phylum	Number of ASVs	Percent Composition (%)
Proteobacteria	1,112	50.4
Marinimicrobia	327	14.8
Firmicutes	199	9
Bacteroidetes	109	4.9
Actinobacteria	100	4.5
Chloroflexi	96	4.3
Nitrospinae	66	3
Acidobacteria	56	2.5
Verrucomicrobia	40	1.8
Planctomycetes	33	1.5
NA (Kingdom:Bacteria)	20	0.9
Gemmatimonadetes	18	0.8
AncK6	9	0.4
Dependentiae	6	0.3
Cyanobacteria	6	0.3
Lentisphaerae	5	0.2
Fusobacteria	2	0.1
Margulisbacteria	1	0
PAUC34f	1	0
Nitrospirae	1	0
Total (Bacteria)	2,207	100
Thaumarchaeota	341	77.1
Euryarchaeota	87	19.7
Nanoarchaeaeota	14	3.2
Total (Archaea)	442	100

Table 6. List of classes that were categorized as Others in Figure 4, and the associated phylum for each class.

Class	Phylum
Anaerolineae	Chloroflexi
Babeliae	Dependentiae
BD2-11 Terrestrial Group	Gemmatimonadetes
BD7-11	Planctomycetes
Brocadiae	Planctomycetes
Fusobacteriia	Fusobacteria
JG30-KF-CM66	Chloroflexi
Lentisphaeria	Lentisphaerae
Melainabacteria	Cyanobacteria
Negativicutes	Firmicutes
Nitrospira	Nitrospirae
OM190	Planctomycetes
Phycisphaerae	Planctomycetes
Pla3 Lineage	Planctomycetes
Subgroup 15	Acidobacteria
Subgroup 21	Acidobacteria
Subgroup 26	Acidobacteria
Subgroup 5	Acidobacteria
Subgroup 6	Acidobacteria
Thermoleophilia	Actinobacteria
Halobacteria	Euryarchaeota
Marine Benthic Group A	Thaumarchaeota

Table 7. Most abundant genera at each depth from the *in situ* rock samples.

Depth in mbsf (sample name)	Most Abundant Genera
10.73 (2R)	All genera were only classified to a higher taxonomic level
13.91 (3R)	All genera were only classified to a higher taxonomic level
26.91 (4R)	Pseudoalteromonas, Halomonas
44.49 (6R)	NS4 Marine Group (Family: Flavobacteriaceae), Pseudoxanthomonas, Granulicatella, Brevibacillus, Methylobacterium
64.52 (8R)	Catenococcus, Pseudohongiella, Gemella, Erwinia
91.29 (11R)	All genera were only classified to a higher taxonomic level
111.98 (13R)	Alteromonas, Nitrospina, Tenacibaculum
119.72 (14R)	Nitrospina, Alteromonas, Alcanivorax, Clade lb (Class: Alphaproteobacteria)
160.53 (18R)	Clade Ib (Class: Alphaproteobacteria), OM27 Clade (Family: Bdellovibrionaceae), Coraliomargarita, Candidatus Scalindua
168.37 (19R)	Capnocytophaga, Nitrospina, Vibrio
182.44 (21R)	Sediminibacterium, XY R5 (Family: Alteromonadaceae), Halomonas, Prochlorococcus
201.59 (23R)	Nitrospina, Halomonas, Candidatus Nitrosopumilus, Alicycliphilus
209.04 (24R)	All genera were only classified to a higher taxonomic level
228.68 (26R)	Tenacibaculum, Rhodopirellula, Halomonas, Alteromonas
241.09 (27R)	Catenococcus, NS2b Marine Group (Family: Flavobacteriaceae), Sulfitobacter, SUP05 Cluster (Family: Thioglobaceae)
247.71 (28R)	Clade Ib (Class: Alphaproteobacteria), Nitrospina, Candidatus Nitrosopelagicus, Catenococcus
274.55 (31R)	Kytococcus, Actinomyces, SUP05 Cluster (Family: Thioglobaceae), Prevotella
285.43 (32R)	Clade Ib (Class: Alphaproteobacteria), SUP05 Cluster (Family: Thioglobaceae), NS2b Marine Group (Family: Flavobacteriaceae), Rhizobium
299.61 (33R)	Alteromonas, Sva0996 Marine Group (Family: Microtrichaceae), Nitrospina, Pseudoalteromonas
306.65 (34R)	All genera were only classified to a higher taxonomic level
324.97 (36R)	Nitrospina, Marinobacter, Halomonas, Pseudoalteromonas
332.78 (37R)	AT s3 44 (Family: Sneathiellaceae), Pseudoalteromonas, Sva0996 Marine Group (Family: Microtrichaceae), Rhizobium
375.08 (41R)	LS NOB (Family: Nitrospinaceae), Prochlorococcus, AT s3 44 (Family: Sneathiellaceae)
382.69 (42R)	Pseudoalteromonas, SUP05 Cluster (Family: Thioglobaceae), Methylophaga, Halomonas

Table 7 continued

Depth in mbsf (sample name)	Most Abundant Genera
404.92 (44R)	SUP05 Cluster (Family: Thioglobaceae), Nitrospina, NS4 Marine Group (Family: Flavobacteriaceae), Halomonas
420.98 (47R)	All genera were only classified to a higher taxonomic level
432.84 (48R)	Hydrogenispora, Pajaroellobacter, Leucobacter, Haemophilus
452.89 (50R)	Alteromonas, Candidatus Nitrosopumilus, Veillonella, GCA (Family: Lachnospiraceae)
460.4 (51R)	Candidatus Nitrosopelagicus, Marinoscillum, AT s3 44 (Family: Sneathiellaceae), Lautropia
522.73 (58R)	Erythrobacter, Parvimonas, Vibrio
533.45 (59R)	Candidatus Endoecteinascidia, Sva0996 Marine Group (Family: Microtrichaceae)
558.50 (62R)	Acidiphilium, Mesorhizobium, Candidatus Nitrosopelagicus, Coxiella
564.77 (62R5)	Clade Ib (Class: Alphaproteobacteria), Alteromonas, Anaerobacillus, Citreicella
600.51 (66R)	Nitrospina, Clostridium, Sva0996 Marine Group (Family: Microtrichaceae), Sarcina
619.64 (68R)	AT s3 44 (Family: Sneathiellaceae), Candidatus Nitrosopelagicus, Sva0996 Marine Group (Family: Microtrichaceae), Clade Ib (Class: Alphaproteobacteria)
626.26 (69R)	Capnocytophaga, Clade Ib (Class: Alphaproteobacteria)
643.87 (71R)	SUP05 Cluster (Family: Thioglobaceae), AT s3 44 (Family: Sneathiellaceae), Enhydrobacter, Sagittula
682.32 (78R)	Nitrospina, Serratia, Bacillus, Leucobacter
711.34 (80R)	Anaerobacillus, Nitrospina, SUP05 Cluster (Family: Thioglobaceae), Rhizobium
714.86 (81R)	Rhizobium, Anaerobacillus, Halomonas, Pseudomonas
747.73 (84R)	Alteromonas, Mesorhizobium, Anaerobacillus, Nakamurella
756.28 (86R)	Nitrospina, Porphyromonas, Clade Ib (Class: Alphaproteobacteria), Marinoscillum
781.45 (89R)	Clade lb (Class: Alphaproteobacteria), Rhodoferax, Nitrospina, LS NOB (Family: Nitrospinaceae)

Table 8. Richness and diversity of the *in situ* rock samples from each depth. Quartiles were calculated based on the diversity values of samples from all depths. NA represents inverse Simpson values that could not be calculated as they were below the subsampling threshold.

Depth (mbsf)	Richness	Diversity (Inverse Simpson)	Quartiles	Diversity (Inverse Simpson)
10.7	4	NA	Min	10.55
13.9	8	NA	Upper Quartile	94
26.9	28	17.23	Median	69
44.5	19	10.55	Lower Quartile	39
64.5	103	69.34	Max	166.44
91.3	6	NA		
111.9	11	NA		
119.7	136	106.55		
160.5	51	43.81		
168.4	12	NA		
182.4	219	166.44		
201.6	113	76.89		
228.8	122	100.13		
241.1	128	87.24		
247.7	55	41.25		
274.6	40	29.95		
285.4	43	37.21		
299.6	107	92.75		
324.9	72	47.08		
332.8	17	NA		
375.1	13	NA		
382.7	72	59.20		
404.9	168	138.02		
432.8	78	69.24		
452.9	146	112.83		
460.4	109	78.28		
522.7	29	24.66		
533.5	23	NA		
558.5	87	64.24		
564.8	113	89.11		
600.5	159	113.54		
619.6	137	96.12		
626.3	21	NA		
643.9	34	22.27		
682.3	67	56.92		
711.3	160	126.65		

Table 8 Continued

Depth (mbsf)	Richness	Diversity (Inverse Simpson)
714.9	53	30.75
747.7	94	70.57
756.3	45	31.98
781.5	63	41.42

Table 9. Correlation coefficients for diversity (inverse Simpson values) and vein frequency in rock samples for depth ranges of every 100 meters below seafloor.

Pearson Correlation Coefficient, Pe				
Depth Range (mbsf)	**Carbonate Vein Frequency**	**Felsic Vein Frequency**	**Total Vein Frequency**	**Number of Inverse Simpson Data Points**
0-100	NA	NA	NA	3
100-200	0.82	0.99	0.93	3
200-300	0.22	0.16	0.27	7
300-400	1.00	1.00	1.00	2
400-500	0.79	-0.55	0.44	4
500-600	-0.89	0.79	-0.31	3
600-700	NA	0.92	0.92	5
700-800	NA	0.88	0.88	5
All Depths	0.20	0.50	0.56	31

Table 10. Number of ASVs and reads constructed with the initial incubation samples' 16S rRNA data for each depth and treatment, followed by the numbers remaining after removal of ASVs present in the blank PCR control, and numbers remaining after quality control (removal of ASVs that are commonly found in PCR contamination).

Depth (mbsf)	Treatment	Initial		Removal of Blank Controls		Removal of Common PCR Contaminants	
		# of ASV	# of Reads	# of ASV	# of Reads	# of ASV	# of Reads
70.9	NT	5	18455	5	20132	0	0
	C	10	187449	1	139	4	11399
	N	7	49630	2	2866	10	16890
	NP	4	17362	0	0	7	21976
91.3	NT	6	47358	10	20173	0	0
	C	15	130225	2	3226	0	0
	N	8	15368	4	2611	0	0
	NP	9	91289	3	10623	0	0
228.8	NT	14	107651	3	7146	1	2776
	C	9	66564	8	14891	3	1466
	N	13	131856	8	13836	4	2611
	NP	12	85444	6	10528	2	3383
247.7	NT	14	116852	3	8424	1	3786
	C	7	108888	9	19786	0	0
	N	13	70959	7	7473	2	158
	NP	24	169771	17	22601	4	9069
274.6	NT	9	169427	3	9781	7	13870
	C	9	120080	4	6666	2	1642
	N	8	102161	3	4196	3	3995
	NP	10	46249	5	3760	12	12144
332.8	NT	10	58121	2	5760	0	0
	C	6	62209	3	215	0	0
	N	8	129151	3	6131	0	0
	NP	10	99686	4	6152	1	246
420.9	NT	18	212754	15	30984	2	126
	C	22	193256	12	29147	0	0
	N	10	98579	5	4952	1	3243
	NP	15	127907	7	7077	1	1309
460.4	NT	11	109690	0	0	2	324
	C	4	19916	5	9340	4	6649
	N	7	45220	3	8745	2	1532
	NP	12	74394	6	5900	3	1181
626.3	NT	4	29279	3	3035	0	0
	C	8	29058	0	0	0	0
	N	9	57404	4	4605	1	6684

Table 10 continued

Depth (mbsf)	Treatment	Initial		Removal of Blank Controls		Removal of Common PCR Contaminants	
		# of ASV	# of Reads	# of ASV	# of Reads	# of ASV	# of Reads
626.3	NP	14	105605	8	11245	3	960
639.3	NT	12	94059	11	49742	0	0
	C	18	175840	7	10302	1	1483
	N	21	120420	15	18714	1	210
	NP	6	60326	1	2	2	1062
714.9	NT	16	243867	7	11547	3	5564
	C	12	149084	11	32865	7	41549
	N	9	123654	4	14877	11	13146
	NP	12	89021	6	19876	1	2
747.7	NT	10	184963	8	39740	3	7764
	C	13	230018	5	12429	2	588
	N	24	112929	14	20159	0	0
	NP	19	293000	13	42481	3	16611
Blank	Blank Filter	19	45584	0	0	0	0
	Blank Kit	11	11480	0	0	0	0
	PCR Blank 1	5	26966	0	0	0	0
	PCR Blank 2	5	26734	0	0	0	0
	PCR Blank 2	1	1	0	0	0	0
	Total	202*	5293213	173*	594880	94*	215398

*Total ASVs are the number of every unique ASV present for all samples, it is not the cumulative number of ASVs from each depth and treatment.

Table 11. Community composition of all incubation samples on the phylum taxonomic level.

Phylum	Number of ASVs	Percent Composition (%)
Proteobacteria	61	64.9
Firmicutes	13	13.8
Bacteroidetes	5	5.3
Acidobacteria	5	5.3
Deinococcus-Thermus	3	3.2
Cyanobacteria	2	2.1
Planctomycetes	2	2.1
Actinobacteria	2	2.1
Armatimonadetes	1	1.1
Total	94	100

Table 12. Richness and diversity of the incubation samples for each depth and nutrient treatments. NA represents inverse Simpson values that could not be calculated as they were below the subsampling threshold.

Depth	Treatment	Richness	Diversity (Inverse Simpson)
	C	4	2.41
	N	10	8.07
70.9	NP	7	2.65
	C	3	2.68
	N	4	2.53
	NP	2	1.30
228.8	NT	1	1.00
	N	2	NA
	NP	4	1.81
247.7	NT	1	1.00
	C	2	1.52
	N	3	1.56
	NP	12	2.77
274.6	NT	7	2.11
332.8	NP	1	NA
	N	1	1
	NP	1	1
420.9	NT	2	NA
	C	4	1.32
	N	2	1.38
	NP	3	1.24
460.4	NT	2	NA
	N	1	1
626.3	NP	3	NA
	C	1	1
	N	1	NA
639.3	NP	2	1.99
	C	5	1.72
	N	11	3.34
	NP	1	NA
714.9	NT	3	2.25
	C	2	NA
	NP	3	1.73
747.7	NT	3	1.92

Quartiles	Diversity (Inverse Simpson)
Min	1
Upper Quartile	1.25
Median	1.72
Lower Quartile	2.37
Max	8.07

Table 13. Richness and diversity of the incubation samples for each depth (all treatments combined). NA represents inverse Simpson values that could not be calculated as they were below the subsampling threshold.

Depth (mbsf)	Richness	Diversity (Inverse Simpson)	Quartiles	Diversity (Inverse Simpson)
70.9	21	9.16	Min	1.30
228.8	10	5.20	Upper Quartile	2.79
247.7	7	2.84	Median	3.33
274.6	22	3.52	Lower Quartile	3.94
332.8	1	NA	Max	9.16
421.5	4	NA		
460.4	11	2.63		
626.3	4	1.30		
639.3	4	NA		
714.9	21	3.32		
747.8	8	3.34		

Table 14. Richness and diversity of the incubation samples for all treatments (all depths combined).

Treatments	Richness	Diversity (Inverse Simpson)
C	19	7.77
N	30	5.23
NP	41	7.03
NT	17	5.90

Table 15. One-way or single-factor analysis of variance ANOVA for effect of different treatments on the microbial diversity of the incubation samples.

Groups	***Count***	***Sum***	***Average***	***Variance***	***Standard Deviation***	
C	6	10.65	1.78	0.42	0.65	
N	7	18.88	2.70	6.36	2.52	
NP	8	14.50	1.81	0.41	0.64	
NP	5	8.29	1.66	0.37	0.61	
ANOVA						
Source of Variation	***SS***	***df***	***MS***	***F***	***P-value***	F_{crit}
Between Groups	4.57	3	1.52	**0.75**	**0.53**	**3.05**
Within Groups	44.62	22	2.03			
Total	49.19	25				

Table 16. Depths and treatments that were removed from Figure 6 due to having no sequences present after quality control.

Depth	Treatments
70.9	NT
91.3	NT, C, N, NP
247.7	C
332.8	NT, C, N
420.9	C
626.3	NT, C
639.3	NT
747.8	N

Table 17. Most abundant genera from each depth for incubation samples. The genera do not include unclassified genera. Descriptions of the closest known isolated relatives to the ASV sequences from these specific genera are also listed.

Depth	Genera	Description of Closest Isolated Relatives to the ASV Sequences for Each Genera
70.9 (9R)	• *Thermicanus* • *Curvibacter* • *Anoxybacillus*	*Thermicanus aegyptius* from oxic soil, is a fermentative microaerophile (Gößner et al., 1999).
		Curvibacter lanceolatus, previously *Pseudomonas lanceolata* was isolated from well water (Ding and Yokota, 2004).
		Anoxybacillus tepidamans, previously called *Geobacillus tepidimonas*, was isolated from geothermally heated soil from Yellowstone National Park, USA, and is moderately thermophilic (Coorevits et al., 2012; Schäffer et al., 2004)
91.3 (11R)	All are only classified to a higher taxonomic level	
228.8 (26R)	• *Acidovorax* • *Falcirhodobacter* • Plot4-2H12	*Acidovorax soli*, was isolated from soil, no notable physiological processes (Choi et al., 2010).
		Falcirhodobacter halotolerans was isolated from soil, no notable physiological processes (Subhash et al., 2013).
		Plot4-2H12 closest relative is *Rhizorhabdus dicambivorans*, isolated from compost, no notable physiological processes (Yao et al., 2016).
247.7 (28R)	• *Bacillus* • *Massilia* • *Pelomonas*	*Bacillus velezensis*, is a surfactant producing bacteria isolated from rivers (Ruiz-García et al., 2005).
		Massilia eurypsychrophila a facultative psychrophilic bacteria, and *M. psychrophila*, both isolated from ice cores (Guo et al., 2016; Shen et al., 2015).
274.6 (31R)	• *Hydrogenophilus* • *Massilia* • *Craurococcus*	*Hydrogenophilus thermoluteolus* and *H. hirschii*, which are moderately thermophilic aerobic betaproteobacteria.
		Craurococcus roseus, an aerobic bacteriochlorophyll a-containing bacteria isolated from soil (Saitoh et al., 1998).
332.8 (37R)	• *Formosa*	*Formosa arctica* is a chemoheterorophic bacteria isolated from seawater sample from the Arctic Ocean (Kwon et al., 2014).
420.9 (47R)	• *Pelomonas* • *Acinetobacter* • *Halomonas*	*Pelomonas saccharophila*, a nitrogen fixing and hydrogen oxidizing bacteria isolated from mud (Xie and Yokota, 2005).
		Acinetobacter proteolyticus, isolated from soil (Nemec et al., 2016).
		Halomonas sediminis, a halophilic bacterium isolated from salt-lake sediment in China (Huang et al., 2008).
460.4 (51R)	• *Tepidimonas* • *Brevundimonas*	*Tepidimonas fonticaldi*, a slightly thermophilic bacteria isolated from a hot spring (Chen et al., 2013).
		Brevundimonas albigilva isolated from soil (Pham et al., 2016).
626.3 (68R)	• *Bradyrhizobium* • *Delftia*	*Bradyrhizobium japonica*, isolated from soil, no notable physiological processes (Wang et al., 1999).
		Delftia tsuruhatensis, a peptidoglycan-degrading bacterium isolated from freshwater (Jørgensen et al., 2009).

Table 17 continued

Depth	Genera	Description of Closest Isolated Relatives to the ASV Sequences for Each Genera
639.3 (70R)	• *Chroococcidiopsis* • *Altererythrobacter*	*Chroococcidiopsis thermalis*, cyanobacteria isolated from soil, no notable physiological processes (Shih et al., 2013).
		Altererythrobacter marinus, isolated from deep seawater of the Indian Ocean, no notable physiological processes (Lai et al., 2009).
714.9(81R)	• RB41 • *Hydrogenophilus* • *Bacillus* • *Phenylobacterium*	*Brevitalia deliciosa*, which was isolated from soil are chemoorganoheterotrophic mesophiles with a broad pH range for growth.
		Phenylobacterium falsum, isolated from non-saline alkaline groundwater, no notable physiological processes (Tiago et al., 2005).
747.7(84R)	• *Hydrogenophilus* • *Bordetella* • *Bacillus* • *Acinetobacter*	*Bordetella muralis*, isolated from plaster wall of a stone chamber, no notable physiological processes (Tazato et al., 2015).

Table 18. Correlation Coefficient for Average Methane Production at 25 and 60 Weeks for Carbonate and Felsic Vein Frequency

Time	Pearson Correlation Coefficient, Pe	
	Carbonate Vein Frequency	Felsic Vein Frequency
25 Weeks	0.076	-0.008
60 Weeks	0.436	0.495

Table 19. One-way or single-factor analysis of variance ANOVA for effect of different treatments on the methane produced for 25 and 60 weeks.

25 Weeks						
Groups	***Count***	***Sum***	***Average***	***Variance***		
NT	12	0.16	0.0096	7.35E-05		
C	12	0.29	0.024	0.00051		
NT	12	0.13	0.011	0.00015		
NP	12	0.27	0.023	0.00044		
ANOVA						
Source of Variation	***SS***	***df***	***MS***	***F***	***P-value***	***F crit***
Between Groups	0.002117	3	0.00071	**2.41**	**0.079**	**2.82**
Within Groups	0.012873	44	0.000293			
Total	0.01499	47				
60 Weeks						
Groups	***Count***	***Sum***	***Average***	***Variance***		
NT	12	0.33	0.028	0.00083		
C	12	0.26	0.0213	0.0010		
NT	12	0.23	0.019	0.00093		
NP	12	0.15	0.013	0.00091		
ANOVA						
Source of Variation	***SS***	***df***	***MS***	***F***	***P-value***	***F crit***
Between Groups	0.0013	3	0.00044	**0.47**	**0.70**	**2.82**
Within Groups	0.041	44	0.00093			
Total	0.042	47				